CONCEPTUAL DESIGN OPTIMIZATION OF A NANO-SATELLITE LAUNCHER

A THESIS SUBMITTED TO
THE GRADUATE SCHOOL OF NATURAL AND APPLIED SCIENCES
OF
MIDDLE EAST TECHNICAL UNIVERSITY

BY

YUNUS EMRE ARSLANTAŞ

IN PARTIAL FULFILLMENT OF THE REQUIREMENTS
FOR
THE DEGREE OF MASTER OF SCIENCE
IN
AEROSPACE ENGINEERING

MAY 2012

Approval of the thesis:

CONCEPTUAL DESIGN OPTIMIZATION OF A NANO-SATELLITE LAUNCHER

submitted by **YUNUS EMRE ARSLANTAŞ** in partial fulfillment of the requirements for the degree of **Master of Science in Aerospace Engineering Department, Middle East Technical University** by,

Prof. Dr. Canan Özgen _____
Dean, Graduate School of **Natural and Applied Sciences**

Prof. Dr. Ozan Tekinalp _____
Head of Department, **Aerospace Engineering**

Prof. Dr. Ozan Tekinalp _____
Supervisor, **Aerospace Engineering Dept., METU**

Examining Committee Members:

Assoc. Prof. Dr. Sinan EYİ _____
Aerospace Eng. Dept, METU

Prof. Dr. Ozan Tekinalp _____
Aerospace Eng. Dept., METU

Asst. Prof. Dr. İlkay YAVRUCUK _____
Aerospace Eng. Dept, METU

Asst. Prof. Dr. Ali Türker KUTAY _____
Aerospace Eng. Dept, METU

Dr. Mehmet Ali AK _____
Senior Engineer, TEI

Date: 10.05.2012

I hereby declare that all information in this document has been obtained and presented in accordance with academic rules and ethical conduct. I also declare that, as required by these rules and conduct, I have fully cited and referenced all material and results that are not original to this work.

Name, Last name : Yunus Emre, ARSLANTAŞ

Signature :

ABSTRACT

CONCEPTUAL DESIGN OPTIMIZATION OF
A NANO-SATELLITE LAUNCHER

Arslantaş, Yunus Emre
M.Sc., Department of Aerospace Engineering
Supervisor : Prof. Dr. Ozan Tekinalp

May 2012, 78 pages

Recent developments in technology are changing the trend both in satellite design and application of that technology. As the number of small satellites built by experts from academia and private companies increases, more effective ways of inserting those satellites into orbit is needed. Among the various studies that focus on the launch of such small satellites, research on design of Launch Vehicle tailored for nano-satellites attracts special attention.

In this thesis, Multiple Cooling Multi Objective Simulated Annealing algorithm is applied for the conceptual design of Launch vehicle for nano-satellites. A set of fitness functions are cooled individually, and acceptance is based on the maximum value of the acceptance probabilities calculated.

Angle of attack and propulsion characteristics are employed as optimization parameters. Algorithm finds the optimum trajectory as well as the design parameters that satisfies user defined constraints. In this study burnout velocity, and payload mass are defined as objectives. The methodolgy is applied for different design scenarios including multistage, air and ground launch vehicles.

Keywords: Multi-Disciplinary Design Optimization, Launch Vehicle, Nano-satellites

ÖZ

NANO-UYDULAR İÇİN FIRLATMA ARACININ KAVRAMSAL TASARIM OPTIMIZASYONU

Arslantaş, Yunus Emre
Yüksek Lisans, Havacılık Mühendisliği Bölümü
Tez Yöneticisi: Prof. Dr. Ozan Tekinalp

Mayıs 2012, 78 sayfa

Teknolojideki son gelişmeler hem uydu tasarımını hem de bu teknolojinin uygulanmasındaki trendi değiştirmektedir. Akademi ve özel şirketler tarafından üretilen uyduların sayısının artması ile birlikte, bu uyduların fırlatılması için daha etkin yöntemlere ihtiyaç duyulmaktadır. Bu tür küçük uyduların fırlatılması ile ilgili çalışmalar arasında nano uyduların fırlatılması için tasarlanan fırlatma araçları özellikle ilgi çekmektedir.

Bu tezde, Çoklu Soğutma Çok Amaçlı Tavlama Benzetimi algoritması nano uydular için fırlatma aracının tasarım optimizasyonunda kullanılmıştır. Bir takım amaç fonksiyonları bireysel olarak soğutulmuş ve kabul edilme koşulu hesaplanan maksimum kabul olasılığına bağlanmıştır. Hücum açışı ve itki sistemi özellikleri optimizasyon parametleri olarak belirlenmiştir. Algoritma optimum yörüngeyi ve kullanıcı tarafından belirlenmiş kısıtları sağlayan tasarım parametrelerini bulmaktadır. Bu çalışmada fırlatma aracının yakıtının bittiği andaki hızı ve faydalı yük amaç olarak belirlenmiştir. Yöntem çok kademeli olarak havadan ve karadan fırlatılan araçlar için uygulanmıştır.

Anahtar Kelimeler: Multi Disiplin Tasarım Optimizasyonu, Fırlatma Aracı, Nano uydular

To My Parents

ACKNOWLEDGMENTS

Foremost, I would like to express my sincere gratitude to my advisor Prof. Dr. Ozan TEKİNALP for the continuous support of my MSc. study, for his patience, motivation, interest and trust in my research. His guidance helped me in all the time of research and writing of this thesis.

My sincere thanks also goes to Dr. Tamer ÖZALP, for his guidance. I could not have imagined having a better advisor and mentor for my career. I owe my special thanks to him due to opportunities and vision he has provided to me at TÜBİTAK.

I would like to express my gratitude to Dr. Mehmet Ali AK for his valuable contributions to this study. I also would like to acknowledge Dr. Ali AÇIKGÖZ for his support during my education life. I couldn’t overcome the obstacles without his help.

I thank to my colleague Cihan AKSOP who helped me during my studies and contributed to my technical and intellectual thinking with his background.

I thank my fellow friends Onur TARIMCI, Zeynep ÇAKIR, Gökhan AHMET and D. Sinan KÖRPE who devoted their time for the stimulating discussions, their technical support and helpful suggestions and comments about this study.

I also take this opportunity to thank my labmates Sinem IŞIK, Mehmet KATIRCIOĞLU, Sinan EKİNCİ, Tuğba Elmas ÜSTÜN, who kept me going in the early days.

I would also like extend my huge warm thanks to my dear friends Onur Tuna GÜL, Kemal BAYHAN, Batu DEMİR, Ş. Eser KUBALI, Seyfullah AKTAŞOĞLU and Hakan AYDOĞAN for their valuable companionship. They were beside me whenever I needed them.

I also would like acknowledge Esin ALTEN, İlter HALİLOĞLU, S. Sena AKARCA BIYIKLI and my friends at TÜBİTAK-UİDB for their support during my thesis studies and constant moral supply. I am also indebted to Nilgün KAPLAN, Derya KAYA and Ahmet UYAR due to their patience and administrative support for completing this study.

I also would like to thank my friends David Ferrer DESCLAUX, Daniela GRAZIANO, Simone La TORRE, Guerric de CROMBRUGGHE, Valentina DONICI, Alejandro IGNACIO, Mirela CONSTANTIN and Victoria ALONSOPEREZ for the unforgettable moments we have lived together during SSP'11. They showed me that we, space geeks, speak the same language although spelling is somehow different.

Last but not the least, I pay high regards to my family for their sincere encouragement and inspiration throughout my life and lifting me uphill of this phase of life. I owe everything to them. Besides this, I would like to thank people have knowingly and unknowingly helped me in the successful completion of this thesis.

This MSc. Thesis is supported by The Scientific and Technological Research Council of Turkey. I would like to thank TÜBİTAK for its generous support throughout the study.

TABLE OF CONTENTS

LIST OF TABLES

TABLES

LIST OF FIGURES

FIGURES

NOMENCLATURE

A_e	Nozzle exit area
C_A	Axial force coefficient
C_D	Drag coefficient
C_L	Lift coefficient
C_N	Normal force coefficient
C_M	Pitching moment coefficient
C*	Characteristic velocity
c	Speed of sound
f*	Global optimum
h	Altitude
I_{sp}	Specific Impulse
k_i	Penalty coefficients
M	Mach number
m	Mass of launch vehicle
m_t	Launch vehicle total mass
m_p	Total propellant mass
n	Pressure exponent
q	Dynamic pressure
P	Pressure
P_0	Reference Pressure
Pr	Probability acceptance constant
R	Universal gas constant
r_0	Reference burning rate
S_{ref}	Aerodynamic reference area
T	Thrust
V	Total velocity
t	Simulation time
t	Time

λ	Longitude
τ	Latitude
ψ	Heading angle
t_b	Burnout time
t_{case}	Thickness of case
t_{liner}	Thickness of liner
T	Atmosperic temperature
α	Angle of attack
γ	Flight path angle, Specific heat ratio
γ_{air}	Specific heat ratio of air
λ	Step size
η	Impulse efficiency
θ	Pitch angle for missile
ρ	Atmospheric density
ρ_{liner}	Density of liner
ρ_s	Density of case
ρ_p	Density of propellant
σ_{steel}	Yield strength of steel
DPR	Design pressure ratio
FF	Fitness Function
GSD	Ground Sampling Distance
LEO	Low-Earth Orbit
LV	Launch Vehicle
MC-MOSA	Multiple Cooling Multi Objective Simulated Annealing
SA	Simulated Annealing
UMOSA	Ulungu Multi Objective Simulated Annealing

CHAPTER I

INTRODUCTION

1.1 Purpose

Design of space vehicles is a multi-disciplinary process. In such a complex process, optimization techniques are essential to choose the initial design point for the vehicle configuration which satisfies the requirements. These optimization techniques should be able to take the requirements and constraints into consideration and evaluate design points from the view of different disciplines. The result from optimization process forms a baseline for the further detailed vehicle designs.

The purpose of this study is to apply Multi-Criteria Multi-Objective Simulated Annealing (MC-MOSA) algorithm for the design of a launch vehicle for nanosatellites. The algorithm aims to find the optimum trajectory with the optimum design parameters related to aerodynamics and propulsion system of the launch vehicle.

1.2 Literature Survey

Simulated Annealing simulates the physical annealing process. In metallurgy materials are heated and cooled in a controlled environment to achieve certain material properties. When the material is heated its internal energy increases and at atomic level particle velocity increases. The particles form regular crystals and this micro-structures grow in time. When the cooling takes a long time, particles can find the optimum formation in which the energy of the system is minimum. Temperature of the system is cooled and a

new formation is tested. As the temperature decreases the amplitude of the test distance decreases. This continues until temperature cools to a certain value or a user defined objective is achieved. The advantage of the SA is thatparticles move toward more optimal points which eliminates the system to stuck in local minimum. The test point is accepted even if it is worse than the previous point.

Kirkpatrick et. al. gave an overview of Simulated Annealing algorithm and Metropolis procedure and emphasized the importance of the annealing process in multi-objective optimization problems [1]. They tested the simulated annealing algorithm on traveling salesman problems of several thousand cities. Application of SA to physical design of electronic systems is also reviewed.

Belisle et al. developed a SA algorithm called Hide and Seek [2]. The given details and discussion of the algorithm together with some conducted numerical experiments have shown that Hide and Seek is more efficient in two multistart global optimization problems.

Arslan and Tekinalp have applied a trajectory optimization technique, and applied to a trajectory optimization problem of an air-to-surface missile configuration [3]. Several case studies are conducted such as maximum range, minimum time of flight to a given range, minimum weight to a specified range.

Utalay and Tekinalp used SA to find the maximum range, as well as specified range minimum flight time trajectories of an air to surface missile [4]. The specified range minimum weight missile configurations were also found by optimizing both the control parameters as well as engine design parameters such as thrust and burnout time.

Bingöl and Tekinalp proposed improvements to the basic SA algorithm [5]. They used the algorithm to optimize both the design and control variables for multidisciplinary design optimization of a missile, and proposed various improvements to the problem formulation.

Simulated Annealing has recently been adapted for the multi-objecive framework by Ulungu and Teghem [6,7]. This method is called as UMOSA (Ulungu Multi-Objective Simulated Annealing). The idea used in UMOSA algorithm is to convert multidimensional objective problems into mono-dimensional problems using the weighted-sum-scalarizing technique. UMOSA has been further improved and tested by Ulungu et. al. on the Knapsack problem [8].

Karslı and Tekinalp applied MC-MOSA algorithm to several benchmark problems [9]. The MC-MOSA method is Elliptic fitness functions are formed to obtain non-convex Pareto fronts. Moreover the quality metrics is formed as a method for the assessment of solutions. They also find the optimum trajectory of an advanced launch vehicle by optimizing angle of attack set during the launch.

There are only few multi-objective algorithms based on Simulated Annealing in the literature. Hence, there is a need to develop SA based multi-objective optimization algorithms.

1.3 Scope

This study investigates nano satellite launchers from different perspectives. In Chapter 2 the question of “why nano launchers” is answered. Some historical and statistical data about launchers is given to pursue reader that although small satellite technology evolved in the past few decades, the development of nano-launchers were not parallel to this breakthrough. Implications of use of this technology is also discussed in this Chapter.

Chapter 3 gives some background information about current studies about nano-launch vehicles. A basic orbital decay analysis is performed to find the target altitude of the nano-launcher. This chapter also deals with the initial sizing of the nano launch vehicle and dynamic model of the launcher. Propulsion model, stage analysis and initial weight calculations are included. Moreover aerodynamic coefficients and initial sizing of different launch vehicle configurations are mentioned in this Chapter.

Chapter 4 gives information about the multi criteria multi objective simulated annealing. It includes basic formulation and introduces the algorithm used in this study.

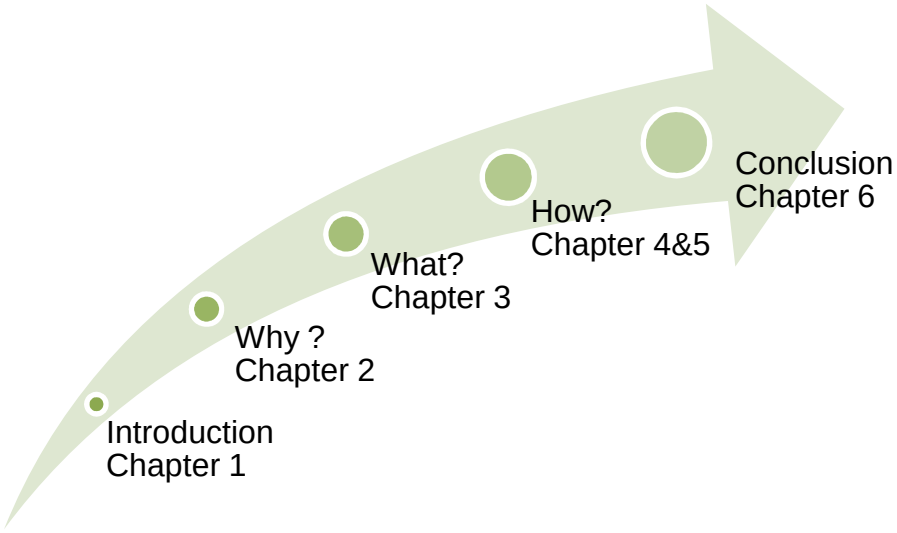

Figure 1-1 General Outline of the Study

In Chapter 5, the results and plots for different nano launcher configurations are given. Some discussion about different design conditions are included in this chapter. Air and ground launch options as are compared in this chapter. The effect of number of fitness functions used in the analysis is included with Pareto-optima front plots.

Chapter 6 concludes this study with suggested future work. It also gives some basic information about the past and future trend of constructing such launch vehicle.

Appendix A includes a sample Matlab code to be used in similar studies. Appendix B describes the methodology used for baseline sizing of the launch vehicle with an example.

CHAPTER 2

SMALL SATELLITES & LAUNCH VEHICLES

The space race between USA-USSR was the driving factor for the earlier space research. Both countries aimed to send first satellite in outer space. The first satellite launched from former USSR Sputnik-1 had a mass of 83,6 kg [10]. The first satellite send by USA was weighing only 13,97 kg [11] . These satellites were equipped with primitive sensors compared to todays technology and aim to observe the conditions at space.

After their maiden flight to space, space faring countries allocated large budgets to build their national space infrastructure. Those countries defined ambitious goals to achieve. Size of satellites increased because more complicated missions tried to be achieved which required state of the art technology. More sophisticated and competent satellites were designed. Complexity and demanding missions resulted in satellites to have a large and heavier structure.

As the technology progressed, more governments and universities become a player in space arena. Between the date of first satellite launch to 2009 more than 6085 satellites were launched by 36 different countries [12]. However as the technology improved the size of electronic components decreased. With the increasing interest to space technology the price of the satellite sub-systems also decreased. Number of research centers and universities started to design and build affordable satellites. New standards for small satellites were introduced. In addition, many private companies

started to offer commercial off the shelf products to those research centers and universities. Although the number of small satellites were increased, inserting these satellites into orbit may be considered as a problem. Small satellites are launched as a secondary payload of large launch vehicles. There is research about nanosatellite launch vehicles, however there is no dedicated LV build to insert those satellites into orbit.

2.1 Applications and Benefits of Small Satellites

At the end of 1990s a new concept was widely accepted by space community. Researchers at the Stanford University with California Polytechnic State University introduced cubesat standards. There are many reasons why small satellites are widely accepted by the space community. There are reasons why cubesat and small satellites was widely accepted. The advantages of small satellites compared to large satellites are [13-15];

- More frequent mission opportunities
- More rapid expansion of the technical and/or scientific knowledge base
- Highly modular, multi-mission satellite bus designs
- Low-cost and rapid way of demonstrating, verifying and evaluating new technologies and services at space
- Low design, production and launch costs
- Less time required for design, build and testing
- A good hands-on experience for future space engineers

Although satellites are small with the available technology they can perform some specific missions. These are:

- Mapping
- Forestry
- Agriculture
- Disaster monitoring
- Geology, Oceanography, Hydrology
- Ship tracking
- Forest Fire Detecting
- Position Location

- Atmospheric Sounding
- Data Collection from Automatic Stations
- Measuring Space Debris

2.2 Current Level and Future Projections for Small Satellite Technology

As a matter of fact, technology allowed small satellites to be used in earth observation as well as scientific missions. In the past Landsat-1 satellite was able to achieve a GSD of 80 meters [16]. Today CHRIS, the 14kg/9W hyperspectral imager, has a GSD of 17m at 560 KM [17].

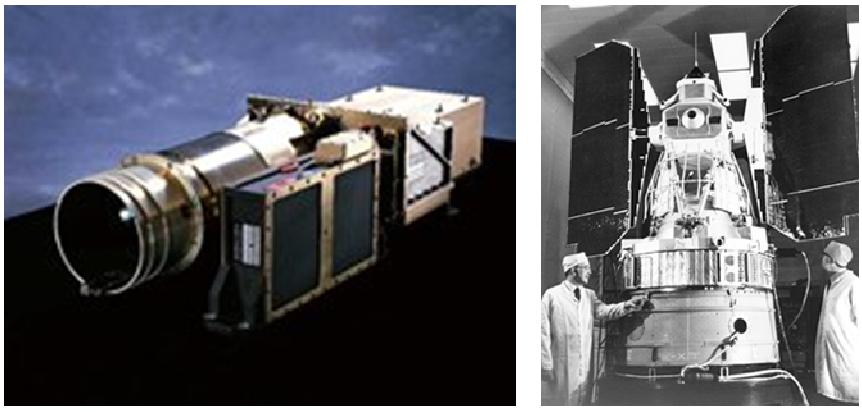

Figure 2-1 Images of Chris and Landsat-1

The first satellites in orbit were powered with batteries. As a result these satellites have a short lifetime. With the use of solar panels the satellites can acquire power needed to perform its operations directly from sun. For example 1 unit cubesat “XI-IV” designed by University of Tokyo can produce 1.1 W. Another example, CanX-2, which is a 3 unit cubesat designed by Toronto Institute for Aerospace Studies’ Space Flight Laboratory is capable of producing 4 W power and is enough to power communication system, attitude control system, GPS receiever, on-board flight computer, imager and scientific payloads.

Some universities and research laboratories are looking ways for practical use of nanosatellites. After these universities launched several

nanosatellites, they aim a higher target. In Japan, University of Tokyo plans to launch a 8 kg nanosatellite which has a capability of obtaining 30m resolution ground images and desired to be used for earth observation [15]. Trends in small satellite community can be summarized as;

- Advances in electronic miniaturization and improvements in the field of optics, mechanics, materials, signal processing, computer technology and communication
- Decreasing cost of the products
- Smaller size and simple design
- Less time required for design, constructing, testing and operating

As a result of the technology, the above mentioned trends boosted the number of small satellites designed.

Satellites that are within the context of this thesis has a weight of between 1-10 kg and launched into orbit successfully. Information about these satellites were obtained from different sources [17,18]. Figure 1 shows the mass of small satellites launched according to the years. It is obvious that number of small satellites were less between 1960-2000. However due to the developments in space technology numbers increased after 2000.

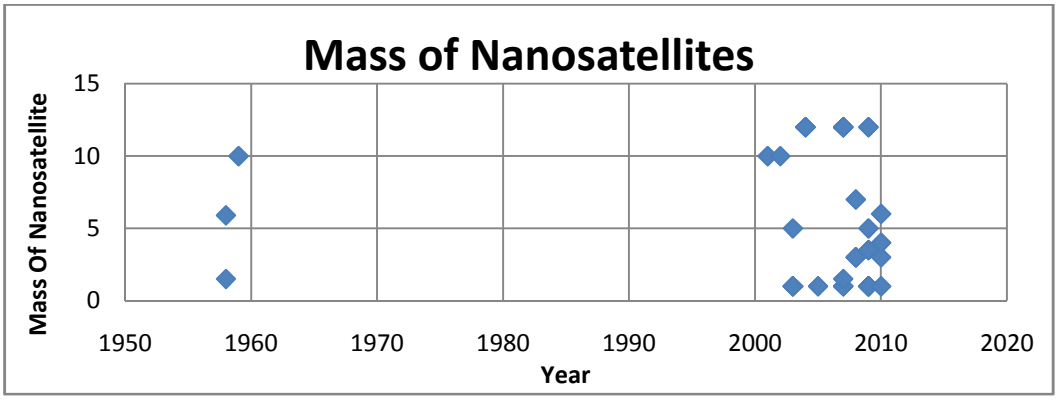

Figure 2-2 Mass of satellites launched according to years

2.3 Current Methods For Launching Small Satellites

Despite the advancements in small satellite technology, number of launch vehicles specifically designed for small satellites is not enough to meet the needs. Small satellites are launched as secondary payload in large launch vehicles and launching satellites in large vehicles causes some problems. First launch time depends on the primary load. It may take more than one year to launch a nanosatellite as primary load and other delays may increase waiting time to launch the vehicle. Second the student graduates and cannot see the result of the work. Third the complexity increases and this may lead to failures.

However there is a large demand for launching small satellites. In the last ten years more than 80 university carried out 125 small satellite research projects. Following 10 launch vehicles are widely used to launch small satellites.

Table 2-1 List of Launch Vehicles and Number of Missions for Nanosatellites

Launch Vehicle	Number of Nanosatellites Launched
Athena-1	1
Dnepr	16
H2A	1
Kosmos 3M	2
Long March 2D	2
Minotaur-I	3
Minotaur -IV	2
PSLV	13
Rokot	6
Space Shuttle	2
Vanguard	3
Total	**51**

Table 2-2 Capacities of Most Widely Used Launch Vehicles

	Mass (Kg)	Number of Stages	Payload
Dnepr	211.000	3/4/5	4500 Kg (LEO)
Rokot	107.000	3	1950 Kg to 200 Km
PSLV	294.000	4	3250 Kg (LEO)
Minotaur-I	36.200	4/5	310 Kg to 740 Km

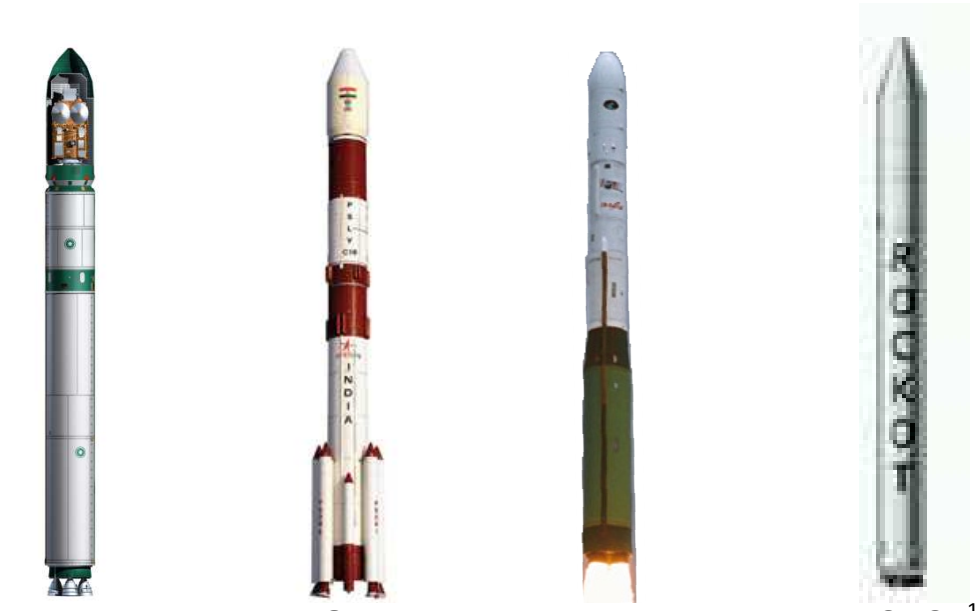

DNEPR PSLV MINITAUR-I ROKOT[1]

Figure 2-3 Most Widely Used Launch Vehicles

Although launch vehicles are used for launching small satellites, the capacity of these vehicles is far more large than putting a single nanosatellite into orbit. Although number of nanosatellites that are built increases every year and there is no dedicated launch vehicle tailored to the needs of small satellite market. The number of satellites planned to be launched is increasing every year. Following figure shows the number of satellites launched in the last 10 years and shows the general trendline.

[1] Images does not reflect actual sizing proportions

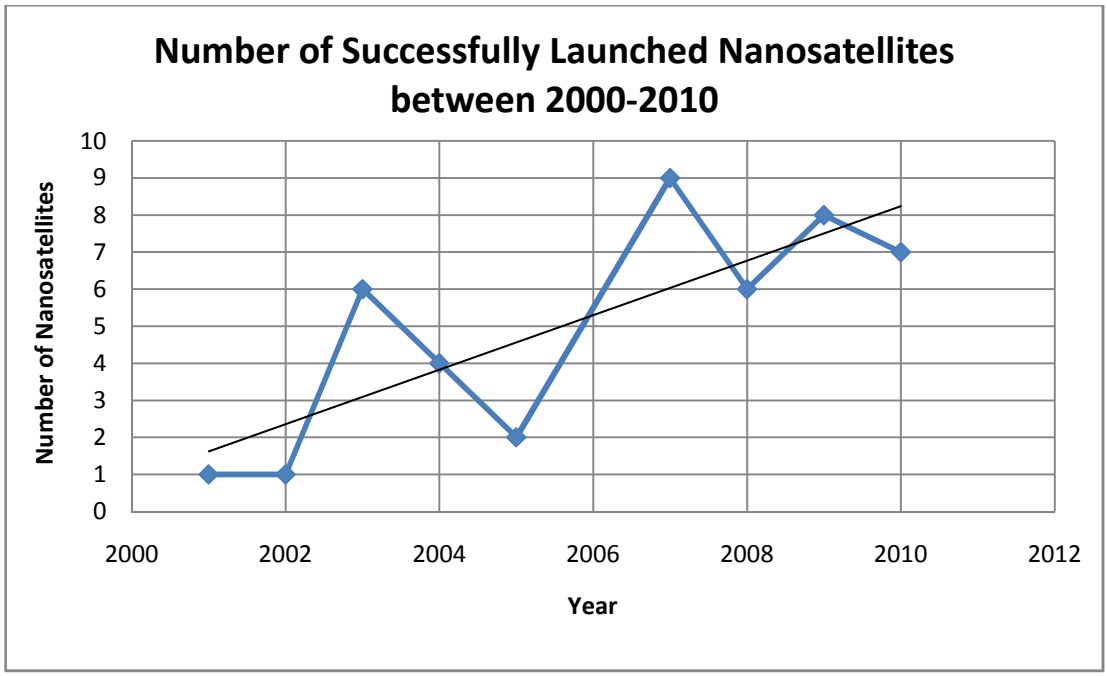

Figure 2-4 Number of Nanosatellites Launched Successfully in the past 10 Years (Total:48)

2.4 Future Small Launch Vehicle Options

There are different options launch vehicle platforms.

2.4.1 Ground Launch

There are different research projects going on around the world. For example Garvey Spacecraft Company is developing a nanosat launch vehicle which is capable of launching nanosat-class small satellites up to Low Earth Orbit. The company is in collaboration with California State University (Long Beach). Ground launch option provides easy access to launch site for preparation phase.

2.4.2 Air Launch

Air launch is another option for inserting nanosatellites into orbit. Generation Orbit Launch Services is a company making research about launching Spacespike-1 (Nanolauncher Blue) and Spacespike-2 (Nanolauncher Black). These launch vehicles can be launched by integrating the system to F-104,

F-15D, Su-27 and F-4. In addition air launching may be considered more economical because it can use high initial velocity, improved thrust efficiency and high expansion ratio of nozzle due to at high altitude. Pegasus and Burlak are operational air launching systems and such systems prove that air launching concept is applicable for launching satellites from aircrafts.

2.4.3 Sea Launch

Sea lunch offers many advantages due to the fact that launch site can be located according to the needs. Launch vehicle may be launched from a ship, a platform or a submarine. For example Shtil is going to be used to launch 50 Cubesats within the context of QB50 mission. Sea launch has advantages due to the fact that platforms are not stationary. The rotational speed of the Earth is greatest at the equator and no extra boost is required to change the inclination of orbit. Moreover, launching a satellite from sea or ocean prevent problems related to a possible failure since it is faraway from populated areas.

Following table includes examples from each option and gives information about cost and capacity of the launch vehicles. However it is obvious that the capacity of the launch vehicles is far more greater than launching a single nanosatellite. For this reason nanosatellites may be launched as a secondary payload, or in constellations.

Table 2-3 Comparison of Capabilities and Cost of Launch Vehicle Options

Launch Vehicle	**Platform**	**Country**	**Capacity kg (lb)**	**Altitude km**	**Estimated Launch Price ($)**
Shtil*	Sea	Russia	430 (947)	200	200.000*
Pegasus XL	Air	US	443 (976)	185	13.500.000
Dnepr	Ground	Russia	4400 (9692)	200	15.000.000
Rockot	Ground	Russia	1850 (4075)	300	13.500.000

*Russian Government subsidizes the cost of the launch vehicle since Shtil is an experimental project.

2.5 Location of Possible Launch Sites

Small launch vehicles do not require complex launch sites and it is easy to perform operations due to reduced complexity. This in turn allows countries to launch vehicles from their territories although they don't have a border to ocean and surrounded by other countries.

- Technical considerations

From technical point of view launching a small satellite does not require a large infrastructure and human resources. Small launch vehicles require less area and less human power. Therefore even developing countries may be able to build small launch site for ground launches. Also Air launch and sea launch options do not require a launch site.

- Geographical Considerations

Normally location of a launch site is an important parameter for launching vehicles.Air launch and sea launch options provide freedom for launching satellites.

- Political Considerations

Access to space is an important factor for countries. There are rationales and benefits of space technology. A country which developed capability to launch a satellite into orbit can increase national prestige. In addition this capability might be used as a tool to develop socio-economic level of the community.

- Judiciary Considerations

Article VII of the Outer Space Treaty provides that the launching state is liable, even if the launch is procured or undertaken by a state's nationals rather than by the state itself. According to Article II of the Liability Convention, the launching state is absolutely liable to pay compensation for

any damage caused by its space object on the surface of the Earth or to aircraft in flight [19]. Considering the above mentioned reasons and technical considerations, a country may launch a nanosatellite launcher within its territories and depending on the design first and second stage might fall to the country's territories. This might eliminate problems related to international space law and regulations [20].

2.6 Future Projections and Implications For the Use of Small Launch Vehicles

Different countries may use nano-launchers for their own needs. For a space faring country national security, increasing scientific and technological knowledge, commercial opportunities, education is the driving factor.

New companies are being established and some of these companies are in close collaboration with universities. Moreover fast Access to space is important from military point of view. Countries might want to obtain information about a region in a very short time and nanolauncher is a valuable tool for responsive Access to space.

Developing countries have different reasons to use nano launchers. These countries want to establish their own space infrastructure. Some countries have cubesat programs and they rely on other launch options. However they can use this system to launch thier own satellites. By achieving this they can increase national prestige. In addition with the increasing capability of nanosatellites they can be used to provide socio-economic benefits to society. Here is a summary list for benefits of small launchers for developing and space faring countries:

Table 2-4 Comparison for Rationales and Benefits of Small Launch Vehicles for Developing and Space Faring Countries

Rationales and Benefits of Developing Small Launch Vehicles	**Developing Countries**	**Space Faring Countries**
National Prestige	**X**	
National Security and Enhancing Military Capability		**X**
Increasing Scientific and Technological Knowledge	**X**	**X**
Space Commercialization		**X**
Provide Benefits to society and assist in social development	**X**	
Training and education	**X**	**X**
Building Space Capabilities	**X**	

Both developing and space faring countries may develop nano launchers for different purposes. With the development of such launchers accessibility to space will increase and more universities, research institutions, companies as well as countries get the benefit of space technology.

CHAPTER 3

MODELLING OF LAUNCH VEHICLE

Dynamic modelling of the launch vehicle is required to obtain the payload capacity and burnout velocity of the vehicle for specific control inputs. First similar vehicles are used as a baseline. However as discussed in the 2nd chapter there is no operational nano-launcher. Therefore the competitive study is rather short. In this chapter details of initial sizing of launch vehicle, dynamic model, engine, number of stage considerations are presented.

3.1 Competitive Study

- AUSROC Nano

The AUSROC Launch Vehicle Program is the most well known research and development program of Australian Space Research Institute. The ultimate goal is to develop a microsatellite launch vehicle utilizing proper technologies may that can be scaled up to be used in heavier launch vehicles [21].

Table 3-1 Specifications of AUSROC Nano

Number of Stages	3
Diameter:	655 mm
Total Length	12.23 m
Delta V	10000 m/s
1st stage	ΔV=2240.88 m/s LOX-Kerosene
2nd stage	ΔV=3459.37 m/s LOX-Kerosene
3rd stage	ΔV=4299.75 m/s Solid Fuel Rocket Engine

- Nano-Launcher

Spaceworks' dedicated NanoLauncher for such satellites is currently being designed to service small satellite launch market [22]. These launchers are based upon multi-stage derivatives of ISAS/JAXA's S-520 solid rocket launched from an existing aircraft such as F-104, F15D, SU-27, F-4.

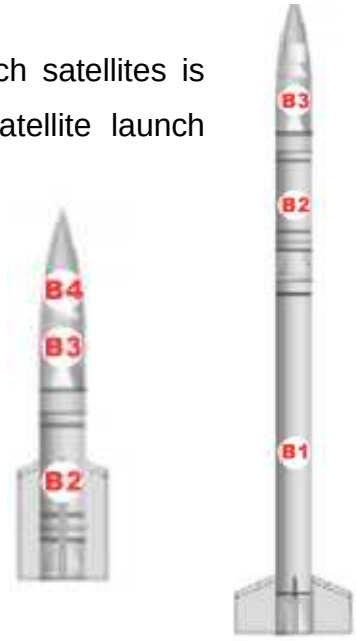

Figure 3-1 Nano-Launcher Blue and Nano Launcher Black

Table 3-2 Specifications of Nano Launcher Blue and Nano Launcher Black

	Nano Launcher Blue	**Nano Launcher Black**
Total Length	5.4 m	10 m
Diameter	0.52 m	0.52 m
Weight	1200 kg	3200 kg
Stages	3	3

- NanoLaunch 1

NanoLaunch is designing, responsive and cost effective vehicle to launch Nano-satellites (1-10 kg) and Micro-satellites (10-100 kg) into Low Earth Orbit (LEO) using the F-15 Eagle as the air platform [23]. Specifications of the launch vehicle are;

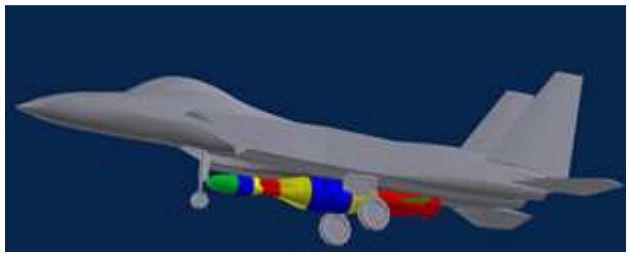

Figure 3-2 Layout of NanoLaunch 1

- Air launched from an F-15
- A two-stage Expendable Rocket Vehicle (ERV) dropped from the airplane
- Paraffin-based/LOX hybrid rockets on both ERV stages
- Restartable second-stage

Table 3-3 General Properties of the NanoLaunch I launch vehicle

Gross weight of ERV stacked with payload hanging on F-15	3,008 kg.
Payload to 400 kilometer polar orbit	30 kg.
F-15 Launch altitude	35,000 Feet
F-15 Launch angle (flight path angle)	300°
F-15 Launch velocity (standard atmosphere)	485 Knots
V provided by 1st and 2nd stage additive to aircraft	8,732 m/s
ERV 1st stage mass	2,771 kg.
ERV 2nd stage mass (excluding payload)	207 kg
Mass contingency carried during performance calculations	15%

- GO1 nano-launcher

Generation Orbit has announced GO1 nano-launcher [24]. GO1 would be an initial demonstrator utilizing mostly existing solid rockets, essentially a minimum viable launch system. GO1 could mature into an operational capability in the 1-10 kg class (LEO payload delivery capability, 250 km circular orbit). However there is no additional information about the design of GO1 nano-launcher.

3.2 Design Parameters:

3.2.1 Altitude:

Nanosatellites have limited lifetime due to mission requirements. Design philosophy of these satellites require them to be desgined to be operational for a shorter period of time due to electronic components and harsh conditions in space.

One of the key parameters of satellite lifetime is orbital decay time if the satellite is launched to low earth orbit. For this study it is assumed that the satellite to be inserted into orbit will decay to the atmosphere after 1 year. For this reason altitude should be estimated. The density of the atmosphere at LEO heights is controlled by solar X-ray flux and particle precipitation from the magnetosphere and so varies with the current space weather conditions.

A simple model for atmospheric density as a function of space environmental parameters is applied to calculate decay rates and orbital lifetimes of satellites in essentially circular orbits below 500 km altitude [25].

Even with a complete atmospheric model describing variations with time, season, latitude and altitude, complete specification of orbital decay is not possible because of uncertainties in the prediction of satellite attitude (which affects the relevant cross-sectional area), and solar and geomagnetic indices (which substantially modify the atmospheric model).

SRMSAT is used for baseline in the atmospheric drag calculations. SRMSAT is a nanosatellite built by students at Sri Ramaswamy Memorial University in India. It was launched by the Indian Space Research Organization's (ISRO) PSLV-C18 launch vehicle in October 2011. The mainframe is 286×286×294 mm^3 in dimension. The mass of the satellite is 10.8 kg with 3 solar panels. It has a design life of one year

After running Matlab Code in Appendix A, it was seen that 10.8 Kg satellite with area of 0.0784 m^2 decays to earth at 370 days when it is launched to a height of 375 km. It is assumed that decay altitude is 180 km.

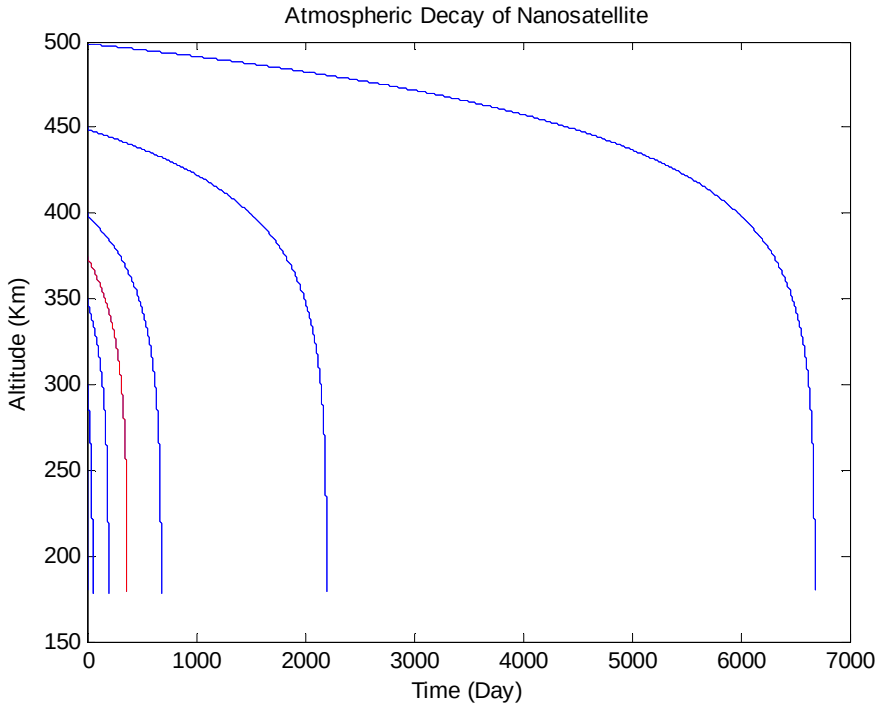

Figure 3-3 Orbital Decay of a Satellite

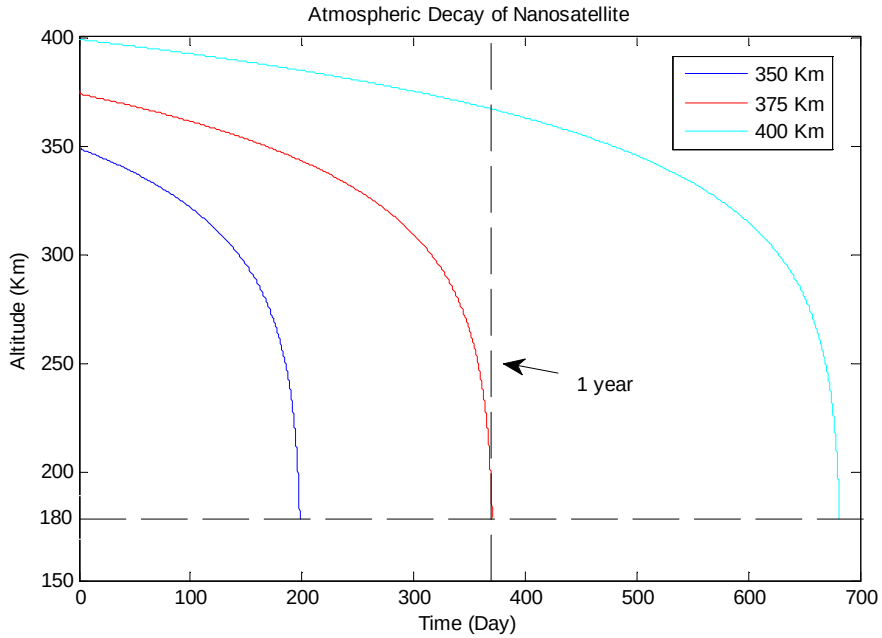

Figure 3-4 Determination of Altitude of a Satellite with 1 Year Decay Time

Table3-4 Altitude versus Decay Time of a Satellite

Altitude	Decay Time (Day)	Decay Time (Year)
200	1,5	0,004
250	12,3	0,03
300	53,1	0,14
350	197,9	0,54
375	**370**	**1,01**
400	681	1,86
450	2201	6,03
500	6682	18,30

Therefore in the initial sizing phase objective altitude will be taken as 375 km. This ensures that the nanosatellite decays to Earth in 1 year.

3.2.2 Launch Vehicle Dynamic Model

The mathematical model for the Launch Vehicle (LV) is obtained from reference [26]. Following assumptions used throughout the simulation;

- The flight mechanics model of LV is given with respect to a rotating, spherical earth with an exponential atmosphere. The model is for 2 stage, liquid-propellant LV.
- US Standard Atmosphere 1976 is assumed for atmospheric calculations.
- No wind or other atmospheric disturbances are included.
- The sideslip and roll angle are assumed to be zero. In this study untrimmed aerodynamics is used. In this case thrust vector (nozzle) gimbal angle is assumed to be zero.

The equations of motion relative to the rotating spherical Earth are given below:

$$\dot{\lambda} = \frac{V\cos\gamma\cos\psi}{r\cos\tau} \quad 3.1$$

$$\dot{\tau} = \frac{V\cos\gamma\sin\psi}{r} \quad 3.2$$

$$\dot{h} = V\sin\gamma \quad 3.3$$

$$\dot{V} = \frac{1}{m}(T\cos(\alpha+\delta) - D - mg\sin\gamma) + r\omega^2\cos\tau(\cos\tau\sin\gamma - \sin\tau\cos\gamma\sin\psi) \quad 3.4$$

$$\dot{\gamma} = \frac{1}{mV}[(T\sin(\alpha+\delta)+L)\cos\mu - mg\cos\gamma] + \frac{V\cos\gamma}{r} + 2\omega\cos\tau\cos\psi + \frac{r\omega^2}{V}\cos\tau(\cos\tau\cos\gamma + \sin\tau\sin\gamma\sin\psi \quad 3.5$$

$$\dot{\psi} = -\frac{1}{mV\cos\gamma}(T\sin(\alpha+\delta)+L)\sin\mu - \frac{V}{r}\tan\tau\cos\gamma\cos\psi + 2\omega(\cos\tau\tan\gamma\sin\psi - \sin\tau) - \frac{r\omega^2}{V\cos\gamma}\cos\tau\sin\tau\cos\psi \quad 3.6$$

$$\dot{m} = -\frac{1}{I_{sp}g_s}\mathrm{T} \quad 3.7$$

Where;

$$L = \frac{\rho_\infty V_\infty S C_L \alpha}{2} \quad 3.8$$

$$D = \frac{\rho_\infty V_\infty S C_D \alpha}{2} \quad 3.9$$

For trimmed aerodynamics, resultant pitch moment due to thrust vectoring is set equal to zero to solve the thrust gimbal angle. Equation for the gimbal angle at trim is;

$$\delta = -\frac{M_A}{Tl_t} \quad 3.10$$

Table 3-5 List of expressions used in the dynamic model of launch vehicle

λ	Longitude
τ	Latitude
h	Altitude above mean sea level
V	Total velocity of the launch vehicle
γ	Flight path angle
ψ	Heading angle
m	Mass of the launch vehicle
$r = r_s + h$	Distance from the center of the Earth to the vehicle mass center
ω	Angular velocity of the Earth
D	Drag
L	Lift
T	Thrust
I_{SP}	Specific Impulse
δ	Gimbal angle of the thrust vector
α	Angle of attack
μ	Velocity roll angle (taken zero in the above equations)

Table 3-6 Initial Conditions

Initial time (t_0)	0 sec
Initial longitude (λ_0)	-80.54 deg
Initial latitude (τ_0)	28.5 deg
Initial altitude (h_0)	0 m
Initial velocity (V_0)	0 m/s
Initial flight path angle (γ_0)	88 deg.
Initial heading angle (ψ_0)	0 deg

Table 3-7 Objectives

Final altitude (h_f)	375,000 m
Final burn-out velocity (V_{if})	≥ V required to achieve R_{earth} + 375,000 m Apogee
Final flight path angle (γ_f)	0 deg
Payload Mass	≥12 kg

RK4 is used to integrate the derivatives.

3.2.3 Atmosphere

The atmosphere is represented by the exponential functions;

Density: $\frac{\rho}{\rho_0} = e^{(\frac{-h}{\lambda_1})}$ Pressure : $\frac{P}{P_0} = e^{(\frac{-h}{\lambda_2})}$

Where the scale-height constants are given by;

$\lambda_1 = 23{,}800\ ft$, $\lambda_2 = 23{,}200\ ft$

And sea-level values of the density and pressure are;

$\rho_0 = 0.002377\ \frac{slugs}{ft^3}$, $P_0 = 2{,}116.24\ \frac{lb}{ft^2}$

Finally, the speed of sound is given by;

$$a = \sqrt{\gamma \frac{p}{\rho}} \tag{3.11}$$

Where $\gamma = 1.4$ is the ratio of specific heat of air.

3.2.4 Aerodynamic Properties

Aerodynamic coefficients is necessary to calculate normal and axial forces as well as moment acting on the launch vehicle. One approach to find the coefficients is using Missile DATCOM™ . In this method the software calls the coefficient at each time step. Alternatively, tables can be formed for different altitude, mach number and angle of attack and required coefficients can be found by interpolation. In this study coefficients are calculated using formulas defined below [27].

The equation for the normal force coefficient body is;

$$|C_N| = [|(a/b)\cos\phi + (b/a)\sin\phi|][|\sin(2\alpha)\cos(\alpha/2)| + 2(l/d)\sin^2\alpha \quad 3.12$$

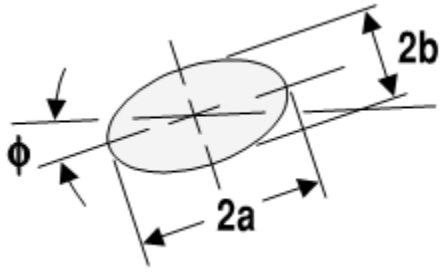

Figure 3-5 Cross section of the Launch Vehicle

The normal force prediction is based on combining slender body theory and body cross flow theory(30). For a launch vehicle $a = b$ and $\phi = 0$. Thus normal force coefficient will be;

$$|C_N| = [|\sin(2\alpha)\cos(\alpha/2)| + 2(l/d)\sin^2\alpha] \quad 3.13$$

Tail,wing and body are the main contributors to drag coefficient and C_D can be expresses as;

$$C_D = C_{D_{Tail}} + C_{D_{Wing}} + C_{D_{Body}} \quad 3.14$$

If each section can be found individually. Drag of tail is sum of skin friction drag and wave drag of tail.

$$C_{D_{Tail}} = C_{D_{Surf\_Tail}} + C_{D_{Wave\_Tail}} \quad 3.15$$

$$C_{D_{Surf\_Tail}} = n_{Tail}\left[0.0133\left(\frac{M}{(qC_{mac})^{0.2}}\right]2\frac{S_{Tail}}{S_{Ref}}\right. \quad 3.16$$

$$C_{D_{Wave\_Tail}} = n_{Tail}\left(\frac{1.429}{\mathrm{M}_{\Lambda LE}^2}\right)\left\{(1.2\mathrm{M}_{\Lambda LE}^2)^{3.5}\left[\frac{2.4}{2.8\mathrm{M}_{\Lambda LE}^2 - 0.4}\right]^{2.5} - 1\right\}\sin^2\delta_{\mathrm{LE}}\cos\Lambda_{\mathrm{LE}}\mathrm{t_{mac}b/S_{ref}} \quad 3.17$$

Similarly drag coefficient of the body is sum of skin friction,base drag and wave drag. This can be expressed as;

$$C_{D_{Body}} = C_{D_{Body\_fric}} + C_{D_{Base}} + C_{D_{Body\_Wave}} \quad 3.18$$

$$C_{D_{Body\_fric}} = 0.053\left(\frac{l}{d}\right)\left(\frac{M}{ql}\right)^{0.2} \quad 3.19$$

If the flight is subsonic, $M > 0.2$ and altitude h<80,000;

$$C_{D_{Base}} = \left(1 - \frac{A_e}{S_{Ref}}\right)(0.12 + 0.13M^2) \quad 3.20$$

If the flight is supersonic;

$$C_{D_{Base}} = \left(1 - \frac{A_e}{S_{Ref}}\right)\left(\frac{0.25}{M}\right) \quad 3.21$$

$$C_{D_{Body\_Wave}} = \left(1.586 + \frac{1.834}{M^2}\right)\left(tan^{-1}\left(\frac{0.5}{l_{nose}d}\right)\right) \quad 3.22$$

C_D is based on Mach number and angle of attack of the launch vehicle. After finding C_D, C_L can be found using following equation;

$$\frac{C_L}{C_D} = (C_N cos\alpha - C_D sin\alpha)/(C_N sin\alpha + C_D cos\alpha) \quad 3.23$$

For the moment coefficient a polynomial equation based on two characteristic parameters, angle of attack and velocity for a similar missile is used [28]. Since the dynamic pressure is negligible most of the time during the launch, above mentioned methods are not necessary for the 2nd stage of the launch vehicle. During the simulation of the dynamic model, angle of attack is set to be zero when the dynamic pressure is less than 1000 kPa.

$$\begin{aligned} \mathrm{M} = (4\mathrm{x}10^{-12}\alpha^4 + 8\mathrm{x}10^{-10}\alpha^3 - 5\mathrm{x}10^{-10}\alpha^2 + 10^{-7}\alpha + 10^{-8})v^3 \\ + (-4\mathrm{x}10^{-9}\alpha^4 - 2\mathrm{x}10^{-7}\alpha^3 + 5\mathrm{x}10^{-7}\alpha^2 + 6x10^{-4}\alpha \\ + 10^{-5})v^2 + (-3\mathrm{x}10^{-6}\alpha^4 - 7\mathrm{x}10^{-6}\alpha^3 + 2\mathrm{x}10^{-5}\alpha^2 \\ + 1.6x10^{-3}\alpha + 2x10^{-4})\, v \end{aligned} \qquad 3.24$$

3.2.5 Initial Mass

During the flight of a vehicle with mass *m* and which produces thrust *T* and experiences drag *D*, has a velocity of *V* at an angle of γ to the local horizontal. This can be expressed as [29];

$$dV = -gI_{sp}\frac{dm}{m} - \frac{D}{m}dt - g\sin\gamma dt \qquad 3.25$$

Initial mass of the launch vehicle is determined from the ΔV_P which is the propulsive change in velocity and m_{pay} the payload mass to be inserted into orbit.

There are three terms in the calculation of ΔV_p. They represent actual change in velocity (ΔV_A), the change in velocity due to the drag (ΔV_D) and the change in velocity due to gravity (ΔV_G) . ΔV_P can be expressed as;

$$\Delta V_P = \Delta V_A + \Delta V_D + \Delta V_G \qquad 3.26$$

Initial sizing of the launch vehicle will require evaluating each of these terms.

3.2.5.1 Actual ΔV

The actual ΔV is the difference between inertial velocity of the vehicle at rest on a rotating Earth and the inertial velocity at burnout in orbit. To first order, this can be approximated by calculating the orbital velocity required and subtracting from it the Earth's rotational speed at the latitude of the launch site (V_{Earth}). V_{orb}, for low Earth orbit is;

$$V_{orb} = \sqrt{Gm_{Earth}\left(\frac{2}{r} - \frac{1}{a}\right)} \quad 3.27$$

Where r is the distance of the body in orbit from the center of the Earth, and a is the semi-major axis of the orbit. Earth's rotational speed is found by;

$$V_{Earth} = \frac{2\pi r}{t} \quad 3.28$$

And Earth's rotational speed at the latitude of the launch site is;

$$V_{Earth_L} = V_{Earth} \cos \lambda \quad 3.29$$

Thus actual ΔV_A is approximated by;

$$\Delta V_A = V_{orb} - V_{Earth_L} \quad 3.30$$

3.2.5.2 Drag ΔV

Drag when divided by the mass and integrated over time gives the drag loss as follows;

$$\Delta V_D = \int_0^{t_b} \frac{D(t)}{m(t)} dt \quad 3.31$$

The integral is complicated to evaluate, when one does not have a design yet. However, the effect of drag can be approximated by calculating the peak drag accelaration and assuming that this accelaration is constant for some period of time.

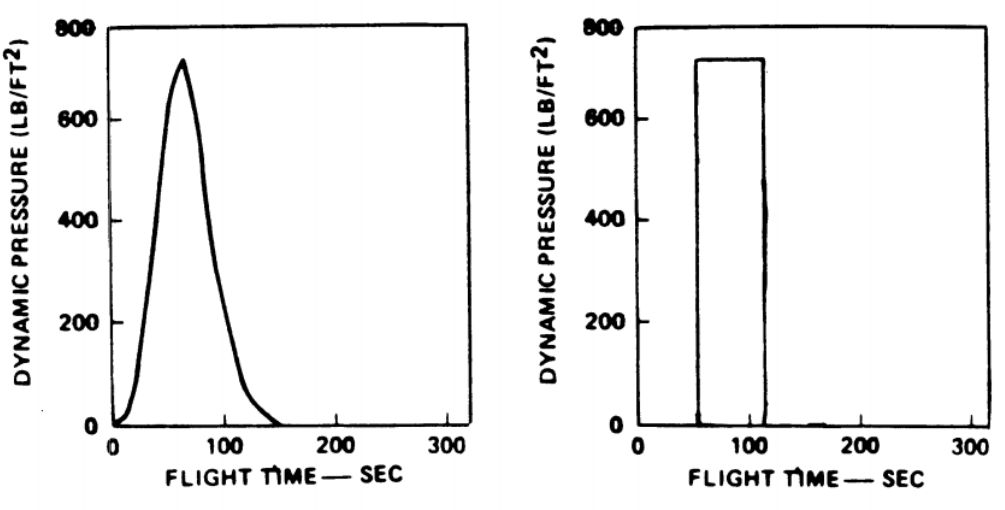

Figure 3-6 Dynamic Pressure History of a Launch Vehicle [29]

$$\Delta V_D = \frac{qS_{ref}C_d}{m} \text{x } t \qquad 3.32$$

Where $\boldsymbol{q}$ is dynamic pressure, $\boldsymbol{S_{ref}}$ is cross-section area of launch vehicle, $\boldsymbol{C_d}$ is the drag coefficient and t is the equivalent duration of maximum dynamic pressure.

3.2.5.3 Gravity ΔV

For a short thrust period t, and neglecting drag, one can integrate equation 3.25 to obtain [29];

$$\Delta V_G = gt\sin\gamma \qquad 3.33$$

Over the course of a flight of duration t_b, this can be approximated as;

$$\Delta V_G \approx gt_b\overline{\sin\gamma} = gI_{sp}\overline{\sin\gamma} \qquad 3.34$$

Where $\overline{\sin\gamma}$ is the integrated average value of $sin\gamma$ over the burn. 30 degree is a reasonable estimate.

Finally after finding ΔV_p following methodology is used to find the initial mass of the launch vehicle.

The mass of a launch vehicle can be broken up into three categories;

1. m_{pay}, the mass of the payload
2. m_{prop}, the mass of the propellant burned
3. m_{struc}, the mass of the structure and everything else (e.g., residual propellant, avionics, etc.)

The sum of these is m_0 , the total liftoff mass. There are two ratios, defined as follows;

$$R = \frac{m_{pay}}{m_{pay} + m_{prop} + m_{struc}} = \frac{m_{pay}}{m_0} \quad 3.35$$

$$\varepsilon = \frac{m_{struc}}{m_{struc} + m_{prop}} \quad 3.36$$

The ratio is referred to as the mass fraction. In addition, define the exponent κ as follows;

$$\kappa = \frac{\Delta V_P}{cn} \quad 3.37$$

where c is the gI_{SP} for each stage and n is the number of stages.
For the entire vehicle (assuming stages of equal I_{SP} and)

$$\frac{\Delta V_P}{c} = n\ln\left[\frac{(1/R)^{1/n}}{\left[(1/R)^{1/n} - 1\right] + 1}\right] \quad 3.38$$

This can be solved for $1/R$ as follows;

$$\frac{1}{R} = \left(\frac{e^{k}(1-\varepsilon)}{1-\varepsilon e^{k}}\right) \qquad 3.39$$

For a given $\boldsymbol{\varepsilon}$ and m_{pay} using the eq. 3.35 initial mass of the launch m_0 vehicle can be found. Appendix B includes a sample calculation.

3.2.6 Number of Stages:

Number of stages can be found by continuing the weight analysis. By calculating 1/R for different I_{sp} and number of stages following table is obtained.

Table 3-8 Effect of I_{SP} and number of stages on Initial Weight of the Launch Vehicle (ΔV_P=10000, ε = 0.15)

	Number of Stages			
$I_{SP}(s)$	1	2	3	4
450	∞	24,36	18,74	17,16
400	∞	42,98	28,69	25,34
350	∞	104,59	51,29	42,54
300	∞	668,46	120,30	87,85
250	∞	1841,7	503,03	264,24
200	∞	∞	17283	1847,4

$^1/_R$ decreases with increasing I_{SP}

$^1/_R$ decreases with number of stages

Given the desired payload mass, the lift of mass of the vehicle found directly. Clearly, the smaller this number, the smaller the overall vehicle.

An I_{SP} of 300 seconds corresponds to that of a vehicle that has a solid propellant engine which tend to have lower I_{SP}. The vehicle which has a liquid propellant engine on the other hand has a lower total lift off weight. Also when the number of stage increase the total weight of the vehicle

decrease. This is due to the fact that, the vehicle does not carry empty fuel tanks all the way to final altitude.

However with the increase in the number of stages complexity increases. Therefore 2 stage launch vehicle is considered to insert payloads into orbit while complexity is reduced. Moreover when Table 3.8 is analyzed for a 3 stage launch vehicle with I_{sp} 350 sec. mass fraction is 1/51.29. This value is may be valid for launch vehicles designed for heavy payloads. But for a nano launch vehicle this is not reasonable. Therefore in this study, initial sizing of 2 stage launch vehicle is done. For the propellant and weight of structure following formulas are used;

$$\Delta V_{total} = \sum_{k=1}^{N} Isp_k \cdot g_k \cdot ln_k \qquad 3.40$$

Where N is the number of stages and $_k$ is the mass ratio of the kth stage.

For 2 stage rocket;

$$\Delta V_{total} = Isp_1 \cdot g_1 \cdot ln_1 + Isp_2 \cdot g_2 \cdot ln_2 \qquad 3.41$$

And;

$$\lambda_1 = \frac{m_{s1} + m_{f1} + m_{s2} + m_{f2} + m_p}{m_{s1} + m_{s2} + m_{f2} + m_p} \qquad 3.42$$

$$\lambda_2 = \frac{m_{s2} + m_{f2} + m_p}{m_{s2} + m_p} \qquad 3.43$$

In this study λ_1 is assigned as optimization parameter. It is related with the staging time. Therefore optimum staging is also applied for the design. Propellant weight of first stage can be found with eq. 3.42 . Moreover weight

of the structure can be found with eq. 3.36 .

Table 3-9 Definition of Staging Expressions

m_{s1}	1st Stage Structural Mass
m_{s2}	2nd Stage Structural Mass
m_{f1}	Propellant Mass of 1st Stage
m_{f2}	Propellant Mass of 2nd Stage
m_p	Payload Mass

3.2.7 Propulsion

There are 3 options for the propulsion system. In this study end burning solid propellant rocket engine and liquid propellant rocket engine is compared. Last option hybrid rocket engine is not included in the analysis.

3.2.7.1 Solid Propellant Rocket

The baseline launch vehicle would be either solid propellant or liquid propellant rocket. First consider the solid propellant case.

For a specified propellant, design pressure, design altitude and for a given thrust and burnout time, there exist only one motor configuration [5]. At the design altitude exit pressure P_e is equal to the ambient pressure P_a and thrust T has maximum value. The variation in ambient pressure by the altitude has a significant effect upon thrust level, which is given by the equation;

$$T = \dot{m}V_e + (P_e - P_a)A_e \qquad 3.44$$

where $\dot{m}$ and V_e are the mass flow rate and velocity of the mass passing through the nozzle exit respectively and A_e is the nozzle exit area. Main parameters for the initial analysis of the solid propellant rocket motor used are illustrated in Table 3.10 .

Table 3-10 Solid Rocket Engine Design Parameters

Parameter	Symbol	Value
Density of Propellant	ρ_p	1765 kg/ m^3
Yield strength of steel	σ_{steel}	1103.5 MPa
Design pressure ratio	DPR	3
Reference burning rate	r_0	0.0089 m/s
Reference Pressure	P_0	13789514 Pa
Pressure exponent	n	0.3
Thickness of liner	t_{liner}	0.002 m
Specific Impulse	I_{sp}	250 s
Gravitational Acceleration	g	9.8 s/ m^2

The relationship between thrust *T* and chamber pressure P_c can be determined due to the fact that the mass of gas produced by the surface must be sufficiently compressed to pass through the nozzle throat. For a given set of motor parameters, the rate of mass produced at the surface is equated to that passing through the throat by equation;

$$\dot{m} = A_b \rho_P r = \frac{P_C \cdot A_{throat}}{C^*} \quad 3.45$$

A commonly used measure of rocket performance, specific impulse, I_{sp}, defined as the ratio of thrust to propellant weight flow per second is given as;

$$I_{sp} = \frac{C}{g} = \frac{\eta \cdot C^* \cdot C_F}{g} \quad 3.46$$

Where g is the gravitational constant, η is the impulse efficiency, C^* is the characteristic velocity, C_F is the thrust coefficient and c is the effective exhaust velocity which is defined by the relationship;

$$C = \frac{T}{\dot{m}} \quad 3.47$$

Hence from previous two equations;

$$\dot{m} = \frac{T}{I_{sp} \cdot g} \tag{3.48}$$

Substituting $r = r_0(\frac{P_C}{P_0})^n$ for an end-burning rocket and equating equation 3.45 and equation 3.48;

$$A_b \rho_P r_0 (\frac{P_C}{P_0})^n = \frac{T}{I_{sp} \cdot g} \tag{3.49}$$

For the left side of this equation, first, for a given chamber pressure, case thikness is calculated to be used in burn area calculation by the help of strength point of view.

$$t_{case} = \frac{P_c \cdot D_{ref} \cdot DPR}{2\sigma_{steel}} \tag{3.50}$$

Then burn area of the end-burning solid propellant rocket motor is calculated with geometric formulation;

$$A_b = \frac{\pi}{4}(D_{ref} - 2t_{case} - 2t_{liner})^2 \tag{3.51}$$

It is assumed that the flow within the nozzle is isentropic and the gas is calorically perfect. Substituting t_{case} value in equation 3.50 into equation 3.51 and A_b value into equation 3.49, P_c can be found for given *T*.

For a launch vehicle of 15 kN GLOW (Gross lift of Weight) and *T/W* of 1.6 required *T* is 24 kN at launch. Using Equation 3.49 and values in the Table 3-10 P_c is found to be approximately 250 MPa. The case is not capable of withstanding the internal pressure resulting from the motor operation. Therefore liquid propelled rocket launch is considered to be more feasible

considering high chamber pressure required in solid propelled rocket engine for generating necessaary *T*. However it should not be concluded that solid propellant rocket engines are not suitable for launch vehicles. There are different motor grain configurations as shown in Figure 3-7. *T* needed to insert satellite into orbit can be achieved by solid propellant rocket engines. However due to reasons described in the next section, in this study liquid propellant rocket engine is used.

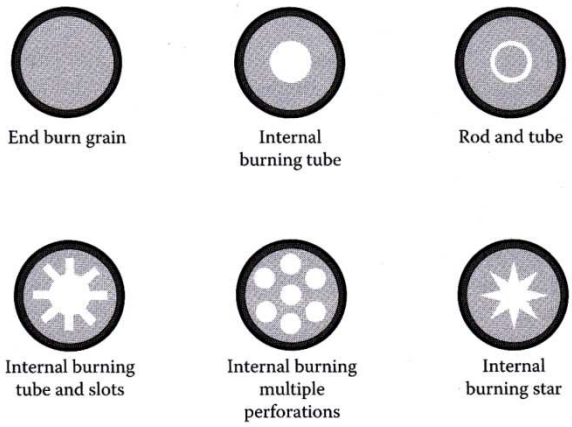

Figure 3-7 Images of Solid Rocket Motor Grain Perforation Configurations [33]

3.2.7.2 Liquid Propellant Rocket

This type of rocket motors use liquid propellants that are fed under pressure into the combustion chamber. In the chamber, the liquid fuel and oxidizer are mixed and burned to form hot gaseous products. They can be shut down and started which is advantagous for space launch. Also thrust level can be adjusted during the operation phase of the engine.

One of the important element is the propellant and the oxidizer. Before sizing the engine type of fuel should be determined. RP-1 (alternately, Rocket Propellant-1 or Refined Petroleum-1) is a highly refined form of kerosene outwardly similar to jet fuel, used as a rocket fuel [30]. Although having a lower specific impulse than liquid hydrogen (LH2), RP-1 is cheaper, can be stored at room temperature, is far less of an explosive hazard and is far

denser. By volume, RP-1 is significantly more powerful than LH2 and LOX/RP-1 has a much better Isp-density than LOX/LH2. RP-1 also has a fraction of the toxicity and carcinogenic hazards of hydrazine, another room-temperature liquid fuel. Thus, kerosene fuels are more practical for many uses.

RP-1 is used in the first-stage boosters of the Soyuz-FG, Zenit, Delta I-III, Atlas, and Falcon 9 rockets. It also powered the first stages of the Energia, Titan I, Saturn I and IB, and Saturn V.

Table 3-11 Specifications of RP-1

Optimum Oxidizer to Fuel Ratio	2.56
Density	1.02 g/cc
Characteristic velocity C	1,805 m/s
Oxidizer Density	1.140 g/cc
Fuel Density	0.806 g/cc
Specific impulse	353 s

For the engines sizing some of the equations are different for the solid propellant case. Therefore a different methodology is used [31].

Thrust is function of mass flow rate, exit velocity, exit pressure, exit area of the nozzle and ambient pressure. Mass flow rate is assigned as optimization parameter. Other variables can be found by;

Exit velocity;

$$V_e = \sqrt{\frac{2\gamma}{\gamma - 1} \mathrm{R}' \frac{\mathrm{T_c}}{\mathrm{M}} (1 - \frac{P_e}{P_c})^{\gamma - 1/\gamma}} \qquad 3.52$$

Pressure at the nozzle thoat;

$$P_t = P_c (1 + \frac{\gamma - 1}{2})^{-\gamma/\gamma - 1} \qquad 3.53$$

Temperature at the nozzle throat;

$$T_t = \frac{T_c}{1 + \frac{\gamma - 1}{2}} \quad 3.54$$

And nozzle thoat area can be found by;

$$A_t = \frac{\dot{m}}{P_t}\sqrt{\frac{R' T_t}{M\gamma}} \quad 3.55$$

Mach number at the exit of nozzle is;

$$M_e = \sqrt{\frac{2}{\gamma - 1}\left[\left(\frac{P_C}{P_a}\right)^{\frac{\gamma-1}{\gamma}} - 1\right]} \quad 3.56$$

Finally exit area of the nozzle is;

$$A_e = \left(\frac{A_t}{M_e}\right)\left(\frac{1 + \frac{\gamma - 1}{2} M_e^2}{\frac{\gamma + 1}{2}}\right)^{\frac{\gamma+1}{2(\gamma-1)}} \quad 3.57$$

Using the mass flow rate $\dot{m}$,exit velocity V_e , area of the nozzle exit A_e and exit pressure and ambient pressure *T* can be calculated with the following expression.

$$T = \dot{m}V_e + (P_e - P_a)A_e \quad 3.58$$

3.2.8 Angle of Attack Input

An angle of attack command profile is determined using nodes equally spaced in time. A sample profile is given in Figure 3-7. The angle of attack values in each node are actually optimization variables and they are given

some upper and lower bounds in optimization algorithm. The values shown in Figure 3-7 are samples. The first node is the initial angle of attack given to the missile, which is also an optimization variable. The angle of attack command for each simulation loop is found by linear interpolation with time

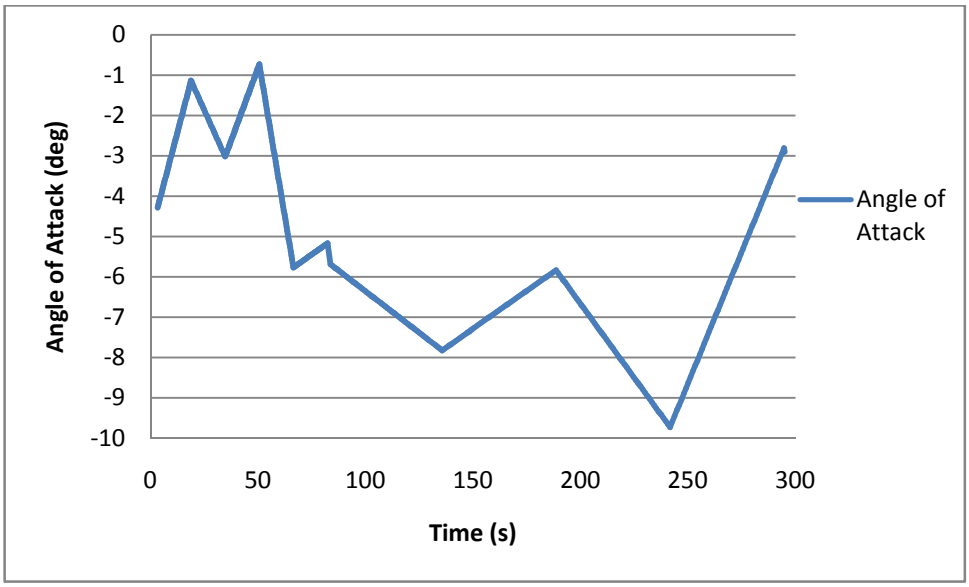

Figure 3-8 Angle of Attack History

3.2.9 Algorithm of Dynamic Model

Step 1

Input listed parameters related to sizing of the launch vehicle

- Total mass
- Propellant mass
- Thrust
- Exit area of nozzle
- Reference area
- Gravitational Acceleration
- Angular velocity of Earth
- Radius of Earth

At this stage set of angle of attack, mass flow rates of 1st and 2nd stage and mass coefficient λ_1 are optimization parameters and comes from the main program.

Step 2

Calculate mass, acceleration, height, velocity, Mach number and heading of the launch vehicle for the first 3 seconds to eliminate singular points.

↓

Step 3 Initialize velocity, heading, latitude, height and longitude

↓

Step 4 Interpolate angle of attack according to simulation time

↓

Step 5 Calculate dynamic pressure

↓

Step 6 Find aerodynamic coefficients for the specific flight phase. Velocity and height is important parameters during the calculations. Also for the 2nd stage coefficients set to be zero. Because the altitude is high enough that the density of the air is very low. This results in low dynamic pressure values although velocity is very high.

Step 7 Equations of motion are integrated

↓

Step 8 Altitude and thrust is updated. Also by calculating consumed propellant, mass of the launch vehicle is updated. At this phase the amount of propellant is checked.

↓

Step 9 Staging occurs when the fuel in the first stage is consumed.

↓

Step 10 Go to step 7 until all propellant is consumed.

↓

Step 11	Return altitude, velocity, inclination angle, latitude and longitude to optimization subroutine

3.3 Investigation of Different Launch Scenarios

In this study 2 different launch scenarios are applied in the design of launch vehicle. In the first case the nano satellite is launched with a launch vehicle from a ground launch base. In other scenario the launch vehicle is loaded onto a F-4 fighter plane and launched at a certain altitude with an initial velocity. It is obvious that when the vehicle is launched from an aircraft it will have an initial velocity which reduces the contribution of vehicles propulsion system for the needed ΔV to achieve objectives. Moreover the dynamic pressure will decrease to negligible level in a shorter time which decreases drag and ΔV needed.

3.3.1 Ground Launch

After calculations the baseline given in Table 3-12 is selected for ground launch vehicle. Example calculations is shown in Appendix B;

Table 3-12 Ground Launch Vehicle Design Configuration

Gross Launch Overall Weight	1958,84 kg
ΔV Reqired	9190,98 m/s
ε	0.18
Payload Mass	11 kg (Satellite + Adapter)

3.3.2 Air Launch

For the 2nd scenario launch vehicle is launched from F-4 with a velocity of 0.8 M and at an altitude of 15,000 m. The baseline used in the optimization procedure is shown in Table 3.13.

Table 3-13 Air Launch Vehicle Design Configuration

Gross Launch Overall Weight	1485 kg
ΔV Reqired	8954.87 m/s
ε	0.18
Payload Mass	11 kg (Satellite + Adapter)

CHAPTER 4

MULTI-OBJECTIVE OPTIMIZATION

Optimization refers to the selection of a best element from some set of available alternatives. This can be achieved by calculating the values of objective function given a defined domain for different inputs which maximizes (or minimizes) the solution.

In this chapter, the Multi criteria multi objective simulated annealing (MC-MOSA) algorithm will be introduced.

4.1 Pareto Optimality

The Swiss economist Pareto introduced Pareto optimality, at the turn of the previous century. To illustrate the meaning of Pareto optimality, the concept of domination should be cleared [9].

In multi-objective optimization algorithms where concept of domination is used, all solution pairs compared with each other on the basis of whether one dominated or not.

In the minimization case, a solution x_1 is said to dominate the other solution x_2 for n objectives, if the below conditions are satisfied together;

- The solution $x_1$is no worse than x_2 in all objectives, or $f_j(x_1) \leq f_j(x_2)$ for all $j = 1, \ldots . M$
- The solution is strictly better than x_2 in at least one objective, or $f_i(x_1) \leq f_i(x_2)$ for at least one $i = 1, \ldots . M$

If any of the above conditions are not violated, then solution x_1 dominates the solution x_2 .These concepts may be clarified in Figure 4.1;

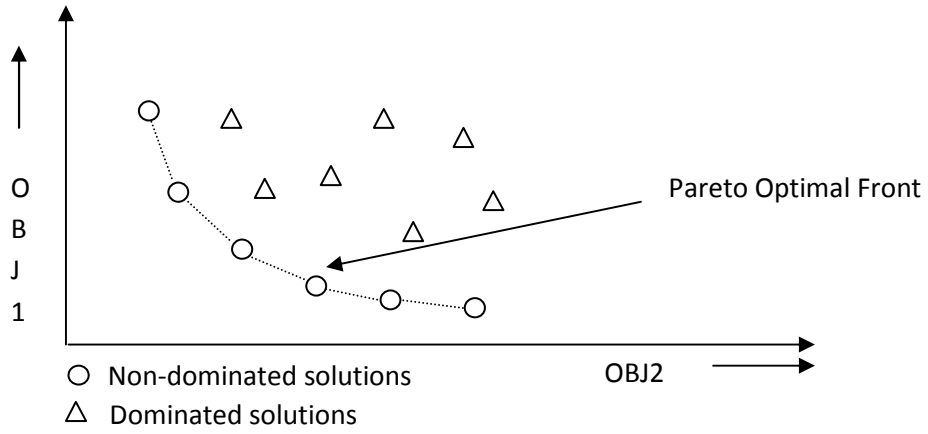

Figure 4-1 Concept of Non-Domination

Multi-objective optimization algorithms try to find the set of solutions, that are non-dominated with respect to each other. This particular set has a property of dominating all other solutions that do not belong to this set. In other words, the members of this set are better compared to the rest of solutions. Then name of this set called non-dominated set. For the case of Figure above, non-dominated points are shown and they are the members of the non-dominated set.

The solutions in the non-dominated set are also named differently as Pareto-optimal solutions. In simple words, a multi-objective optimization solution x is Pareto-optimal if it can not be improved in any objective $f_i(x)$ without causing a degradation in at least another objective $f_j(x)$. Then, for a multi-objective optimization algorithm, it is desirable to find all the Pareto-optimal solutions so that user can select the best one based on his preference.

4.2 Multi-Objective Optimization Problem

In this study Multiple Cooling-MOSA MC-MOSA is applied to 2 different aerospace design problems. In MC-MOSA many fitness functions are used in parallel [31]. Temperature of each fitness function is cooled individually.

Acceptance of the points is based on a probabilistic function. If the solution is accepted than the temperature is cooled. When the temperature is decreased the distance of random walk also decrease and solution converge to global minimum. Use of probability acceptance criteria assures that the solution does not converge to local minimum.

4.3 Multiple Cooling- MOSA Method

Algorithm of Multiple Cooling-MOSA procedure is as below and in the algorithm N is the number of the objectives and M is the number of the fitness functions;

Step 0:

- Generate initial values
- Generate 1st test point x^0 in the interior of S
- Set temperature vector T^0 of dimension *M* (i.e., number of fitness functions) to high values. Also set initial values of the best and next best records of the FFs to zero. ($\tilde{F}^{best} = \tilde{F}^{nextbest} = 0$)

Step 1:

- Choose a search direction θ^K with uniform distribution on the surface of a unit sphere.
- Choose a step size λ^K such that;
  $\Lambda^{\mathrm{K}} = (\lambda^K \in \mathrm{R};\ x^K + \lambda^K \theta^K \in \mathrm{S})$ set $y^K = x^K + \lambda^K \theta^K$

Step 2:

- Generate V^K $(0 \leq V^K \leq 1)$ from uniform distribution

Step 3:

Evaluate the probability acceptance function

- $Pr = min\left\{1, \max\left[\exp\left(\frac{\Delta\tilde{F}_m^K}{T_m^K}\right)\right]\right\}$
  $\Delta\tilde{F}_m^K = \tilde{F}_m(x^K) - \tilde{F}_m(y^K), \quad m = 1, \dots, M$

Where $\tilde{F}_m$ is a set of elliptic fitness functions.

Step 4:

Perform a test on the the trial point,y^K, and accept it with probability Pr

$$x^K = \begin{Bmatrix} y^K & if\ V^K \in (0, Pr) \\ x^K & otherwise \end{Bmatrix}$$

Step 5:

If $Pr = 1$ (i.e., if there are any better fitness functions, $\tilde{F}_m(y^K)$,($m = 1, \dots, M$)):

1) Archieve the test point $x^{K+1} = y^K$, with values of the objectives, ($f_i(y^K)$), to be reprioritize to obtain the Pareto front.
2) If the test points improve the FFs :
    a. Decrease the temperature of the FFs using:

$$T_m = 2\frac{[\tilde{F}_m(x^{K+1}) - \tilde{F}_m^*(y^K)]}{\chi^2_{1-p}(d)}$$

In this formula $\tilde{F}_m^*$ is the global minimum of the *m*th FF, and $\chi^2_{1-p}(d)$ is the 100(1-*p*) percentile point of the chi-square distribution with d degrees of freedom. Since global minimum is not known in advance, its estimate $\tilde{F}_m^e$ is used instead where ;

$$\tilde{F}_m^e = \tilde{F}_m^{best} + \frac{\tilde{F}_m^{best} - \tilde{F}_m^{nextbest}}{(1-p)^{-d/2} - 1}$$

The estimator may also be used with upper and lower bounds as well:

$$\tilde{F}_m^* = \begin{Bmatrix} \tilde{F}_m^{lower} & if\ \tilde{F}_m^e < \tilde{F}_m^{lower} \\ \tilde{F}_m^{upper} & if\ \tilde{F}_m^e > \tilde{F}_m^{upper} \\ \tilde{F}_m^e & otherwise \end{Bmatrix}$$

Step 6:

Increase the loop counter and go to Step 1 and continue to evaluate function values until permitted number of function evaluations is completed.

Step7:

To get a set of solutions that approximates the actual Pareto front, carry out a non-dominated sorting algorithm from the results archived in Step 5.

In the following section special elliptic FFs are introduced which have a good performance in capturing non-convex fronts.

4.4 Elliptic Fitness Function

Elliptic fitness functions are constructed to capture non-convex Pareto Optimal front using the methodology described in reference [32]. Consider an ellipse centered at $C(\tilde{f}_1^C,\ \tilde{f}_2^C)$, while semimajor and semiminor axis are in line with the coordinate directions. Semimajor axis of ellipse may be written as Eq. 4.1 the ellipse passes through point $P(\tilde{f}_1^P,\ \tilde{f}_2^P)$, :

$$a = \sqrt{(\tilde{f}_1^P - \tilde{f}_1^C)^2 + \kappa(\tilde{f}_2^P - \tilde{f}_2^C)^2} \qquad 4.1$$

where, $\kappa = 1/(1-e^2)$, and e is the eccentricity of the ellipse. The semi major axis of this ellipse may be written in Eq. 4.2 provided that the semimajor axis is aligned with a line connecting ellipse center C to point $G(\tilde{f}_1^G,\ \tilde{f}_2^G)$:

$$a = \sqrt{\mathrm{r^T Q^T \Lambda Q r}} \qquad 4.2$$

where,

$$r = \left\{\tilde{f}_1^P - \tilde{f}_1^C, \tilde{f}_2^P - \tilde{f}_2^C\right\},\ \mathrm{Q} = \begin{bmatrix} \cos(\varphi) & \sin(\varphi) \\ -\sin(\varphi) & \cos(\varphi) \end{bmatrix},\ \Lambda = \begin{bmatrix} 1 & 0 \\ 0 & \kappa \end{bmatrix}$$

φ is the angle between the horizontal axis and the line $\overline{\mathrm{CG}}$ (Fig. 3).

A set of ellipses may be formed by uniformly locating their centers along a quarter circle Fig. 4.2 . Then, the objective is to minimize the semimajor axes of the ellipses (i.e. , $F_j = a_j$). The minimum of each semimajor axis becomes the point closest to a particular center.

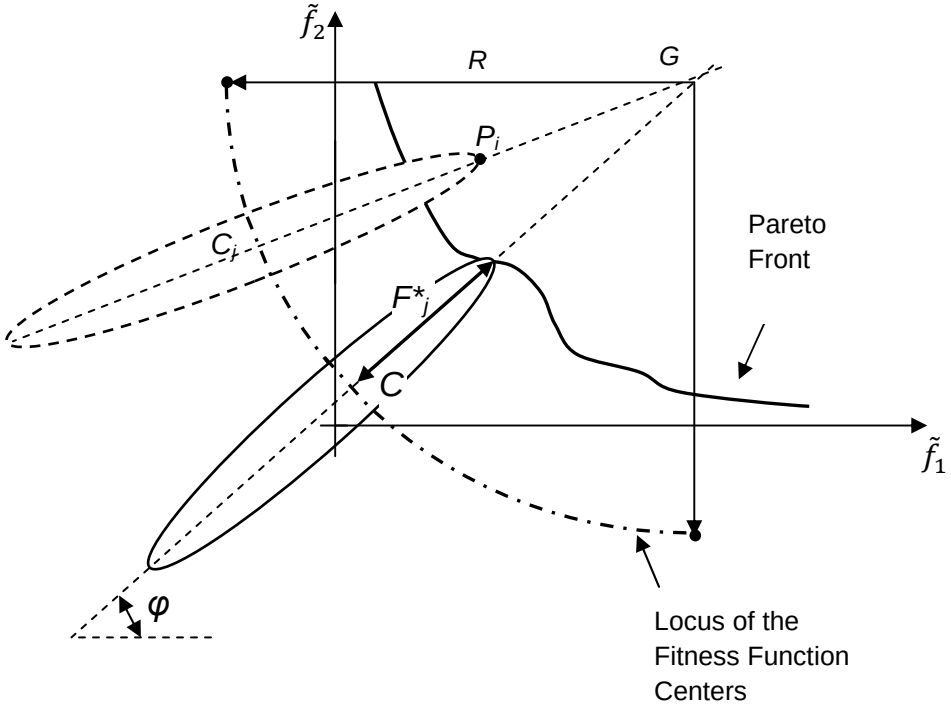

Figure 4-2 Construction of Fitness Functions

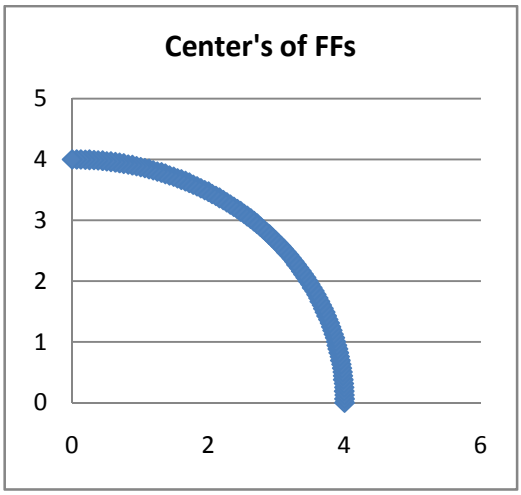

Figure 4-3 Center Location of Elliptic Fitness Functions

4.5 Quality Metrics

In this study, the quality assessment of the non-dominated points obtained through multi-objective optimization are conducted using four metrics

proposed in [32]. They are: accuracy of the Pareto front (AC), cluster (CL). the hyper-area difference (HD) and overall Pareto spread (OS),

The hyper-area difference is the area below the Pareto front, as shown in Figure 4.3 a. If the HD is small, the Pareto front solution set is better.

Overall Pareto spread (OS) is the area of the maximum rectangle bounded by the two extremes of the Pareto front (p_1 and p_2) as shown in Figure 4.3 b. If the solution set is spread between the two extreme points, the area will be larger. Therefore Pareto front with large OS is better than a front with a smaller value.

Accuracy (A) is a measure of smoothness of the Pareto front. The metric is defined as the inverse of areas constructed from neighbouring solutions (Figure 4.3 c) . If the solution set contains all the actual Pareto solutions (i.e., a continuous Pareto front), then the total area will be zero, causing the AC metric to be infinite. Solution set with a large AC is better than the one with smaller AC.

It is desirable to have the solutions spread uniformly along the front. Clustering occurs, when too many solutions are found at certain parts of the front, while other parts are empty. To obtain the CL_{μ} metric, the whole domain normalized objectives is divided into square grids of size μ. In order to have a good spread, each rectangle shall be occupied by a single solution giving a CL_{μ} metric equal to one. For example, in Figure 4.3 d there are three solutions in the front, and three grids are occupied (i.e., $CL_{\mu} = 1$).

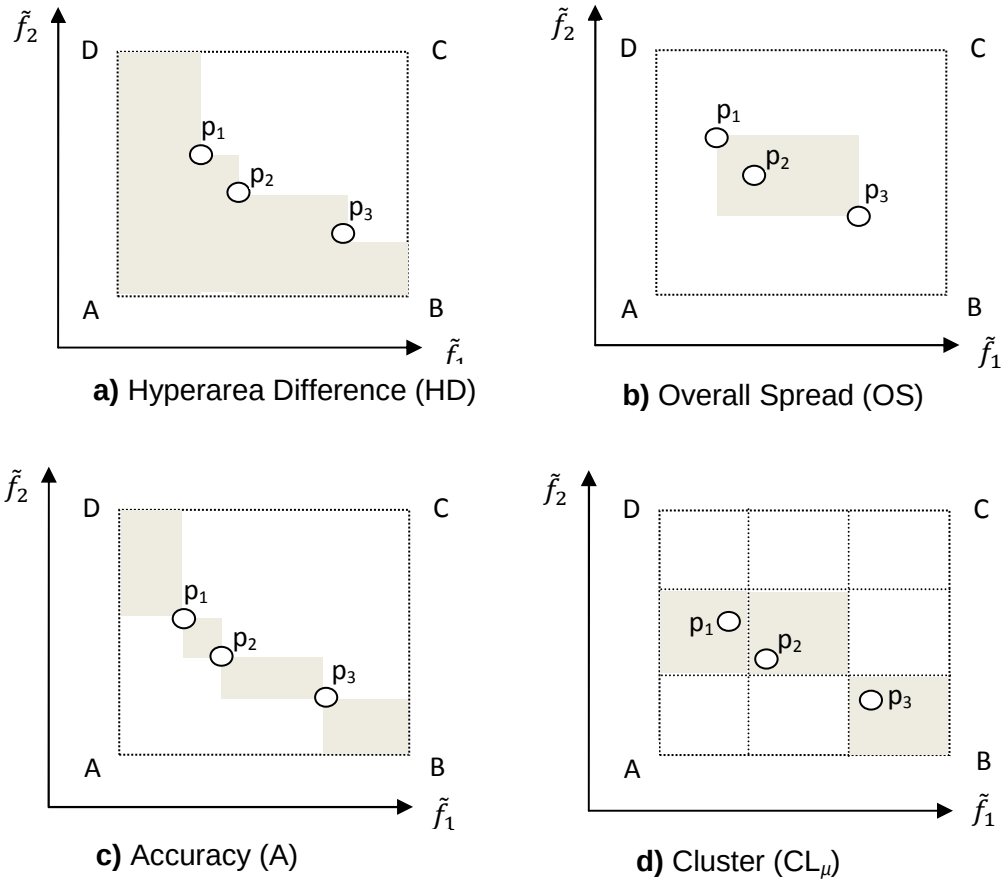

Figure 4-4 Quality Metrics

Results of the optimization phase is shown in Table 4-1. The results are obtained with 10k function evaluation numbers and 100 FFs.

Table 4-1 Quality Metrics

	Hyperarea Difference	Overall Spread	Accuracy	Cluster
Ground Launch	2.22×10^{11}	2.42×10^{7}	4.53×10^{-11}	10
Air Launch	2.01×10^{10}	1.46×10^{7}	4.98×10^{-11}	5

CHAPTER 5

MULTI-OBJECTIVE TRAJECTORY AND LAUNCH VEHICLE DESIGN OPTIMIZATION

In this section optimization algorithm which is defined in Chapter 4 is applied to 2 different launch vehicle configurations given in Chapter 3.

5.1 Definition of Problem

Launch vehicle design problem posed as a multi-objective optimization problem. The objectives are maximizing altitude and maximizing the final velocity, that is the satellite insertion velocity to the orbit. Initial conditions and terminal conditions are defined in Chapter 3.

Two objectives of maximum altitude and maximum velocity are sought for while the launch vehicle is flown until all available propellant is consumed.

The optimization parameters are the angle of attack values at the nodes, mass flow rate of 1st and 2nd stage, λ_1 which is the mass ratio of launch vehicle before and after propellant of 1st stage is consumed.

Table 5-1 Range of Optimization Parameters

	α	$\dot{m}_1$	$\dot{m}_2$	λ_1
Ground Launch	-10 < α <10	14 < m_1 <15	2.0 < $\dot{m}_2$ <2.2	2 < λ_1 < 4
Air Launch	-10 < α <10	6 < m_1 <8	1.8 < $\dot{m}_2$ <2.0	2 < λ_1 < 5

Angle of attack valus find the optimum path of the launch vehicle. The nodes are equally spaced in time and the angle of attack values between the nodes are obtained by linear interpolation from the neighbouring nodes. In both design scenarios 14 nodes are used. Mass flow rates define the *T* produced. λ_1 defines the staging time. Design and optimization methodology is shown in Figure 5-1.

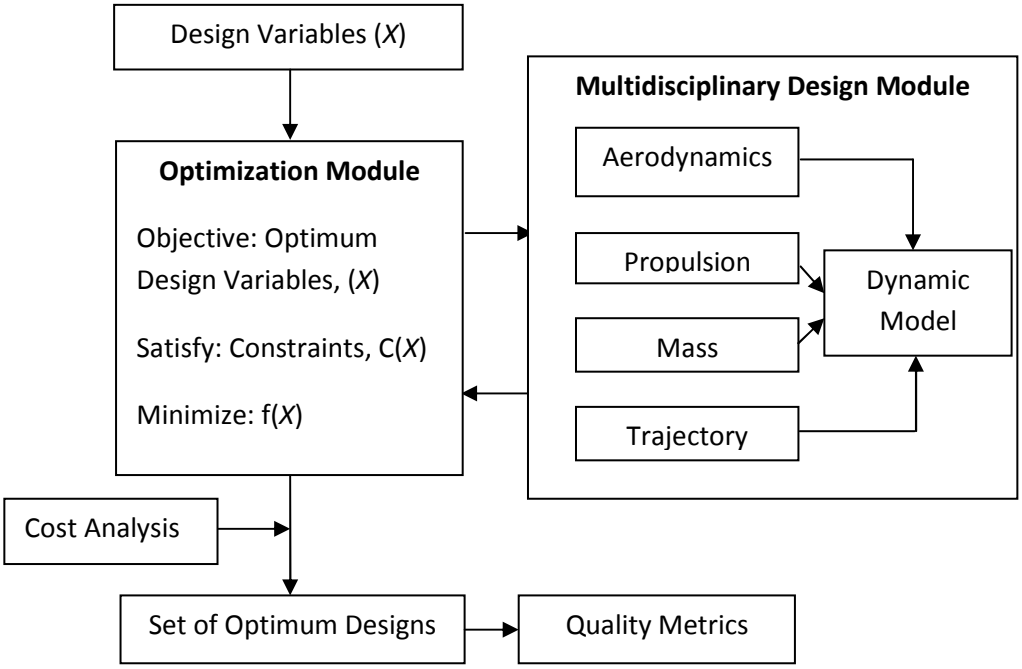

Figure 5-1 Optimization Methodology

Table 5-2 Launch Vehicle Design Objectives

Payload Mass	≥12 kg
Burnout-Velocity	≥V required to achieve R_{earth} + 375 km Apogee

Then the multi objective optimization problem is posed as;

Maximize f_1 = Payload-mass

Maximize $f_2 = V_{burnout}$

Since realizing the equality constraints is a difficult task, they are converted into tight inequality constraints.

$$h_{burnout_f} - \varepsilon_1 \leq h_{burnout}(t_f) \leq h_{burnout_f} + \varepsilon_1$$

$$\gamma_f - \varepsilon_2 \leq \gamma(t_f) \leq \gamma_f + \varepsilon_2$$

$$R_{Apogee_{min}} \leq R_{Apogee_f} \leq R_{Apogee_{max}}$$

Where γ_f is the desired final value of the flight path angle, $\gamma(t_f)$ is the flight path angle at the burnout, $R_{apogee_{min}}$ is R_{Earth}+375 km , $R_{apogee_{max}}$ is R_{Earth}+450 km, R_{Apogee_f} is the value of the apogee at the end of the analysis. In this study $\varepsilon_1 = 5000$ m , $\varepsilon_2 = 1°$. Also consumed reserved propellant mass is penalised.

At orbit insertion flight path angle should be zero ($h_{burnout_f} = 0$). Also it is desired that the optimum configuration consume less propellant to achieve the objectives. In this study target is to maximize the objectives. Then the problem is;

$$z_j = a_j + \Omega \qquad 5.1$$

j= 1, …., N where N is the number of fitness functions and a_j is the semi major axes of the ellipses to the Pareto-Front, and Ω is the cost associated with the constraints. If the consraints are between the desired range, penalty associated with this constraint is taken zero. Hence (if final values of states are greater than maximum limit);

$$\begin{aligned}\Omega = +k_1 \max\left(0, \text{abs}\left(h_{burnout}(t_f) - h_{burnout_f}\right) - \varepsilon_1\right) \\ + k_2 \max\left(0, \text{abs}\left(R_{Apogee_f} - R_{Apogee_{max}}\right)\right) \\ + k_3 \ \left(0, \text{abs}\left(\gamma_{burnout}(t_f) - \gamma_f\right)\right. \\ \left. - \varepsilon_2\right) + k_4 \ \left(m_{reserve\_prop}(t_f)\right)\end{aligned} \qquad 5.2$$

Where $k_1 = 1\text{x}10^{-5}$, $k_2 = 1\text{x}10^{-5}$, $k_3 = 0.1, k_4 = 0.1$ are the penalty coefficients and defined according to the order of magnitude of the constraint.

If penalty coefficient is increased for one particular constraint, a different solution set is obtained where all feasible solutions are strictly lies between the bounds. Objectives, optimization parameters and constraints are defined in the Table 5-3.

Table 5-3 Summary of Objectives, Optimization Parameters and Constraints

Objectives	Optiization Parameters	Constraints
Payload Mass $V_{burnout}$	α (a.o.a at each node) $\dot{m}_1$ and $\dot{m}_2$ λ_1	$h_{burnout}$ R_{Apogee} $\gamma_{burnout}$ $m_{reserve\_prop}$

5.2 Solution

Launch vehicle design optimization problem was solved with MC-MOSA method. In the solution 17 optimization parameters (14 a.o.a, mass flow rate of 1st and 2nd stage, mass ratio) are used. Objective is to maximize burnout velocity and payload mass. Initially the dynamic model is simulated and values of the objectives are obtained at burnout. Constraints are defined such that 145 km ≤ $h_{burnout}$ ≤ 155 km and $-1° \leq \gamma(t_f) \leq 1°$. Certain amount of propellant (20 kg ≤ $m_{propellant}$ ≤ 50 kg) is reserved from propellant of 2nd stage. Reserve propellant is consumed to put the launch vehicle into circular orbit at R_{apogee}. If the reserve fuel is not consumed totally, it is added as payload mass. R_{apogee} is found by following equations;

$$(Rp/r)_{1,2} = (-C \pm \sqrt{C^2 + 4(1-C)sin^2\gamma})/(2(1-C)) \quad (5.3)$$

Where;

$$C = 2Gm/(rV^2) \quad (5.4)$$

Apogee radius is;

$$R_{Apogee} = r(Rp/r)_1 \quad (5.5)$$

γ is the angle between radius vector and velocity vector of the launch vehicle. Reserve propellant is consumed to provide ΔV required to obtain circular orbit when the launch vehicle is at R_{apogee}.

$$\Delta V_{required} = V_{Circular} - V_{burnout} \quad 5.6$$

Where,

$$V_{Circular} = \sqrt{\frac{Gm}{R_{apogee}}} \quad 5.7$$

In order to guarentee that the launch vehicle reaches R_{apogee};

$$V_{burnout} \geq \sqrt{\frac{2Gm}{R_{apogee}} - \frac{Gm}{(R_{apogee} + R_{perigee})/2}} \quad 5.8$$

It should be noted that the dynamic model is not simulated after burnout. Instead above equations are used the find the required velocity and delta-V to obtain circular orbit at R_{apogee} .

5.2.1. Ground Launch

Table 5-4 Final Design Results for ground based Launch Vehicle

Gross Launch Overall Weight	1958 kg
Weight of 1st stage	1452 kg
Weigt of 1st stage fuel	1241 kg
Weight of 2nd stage	506 kg
Weigth of 2nd stage fuel	423 kg
ΔV of 1st stage	3103 m/s
ΔV of 2nd stage	5953 m/s
Seperation Time	78.88 s
Velocity at Burnout	8018.43 m/s
Altitude at Burnout	150,960 m

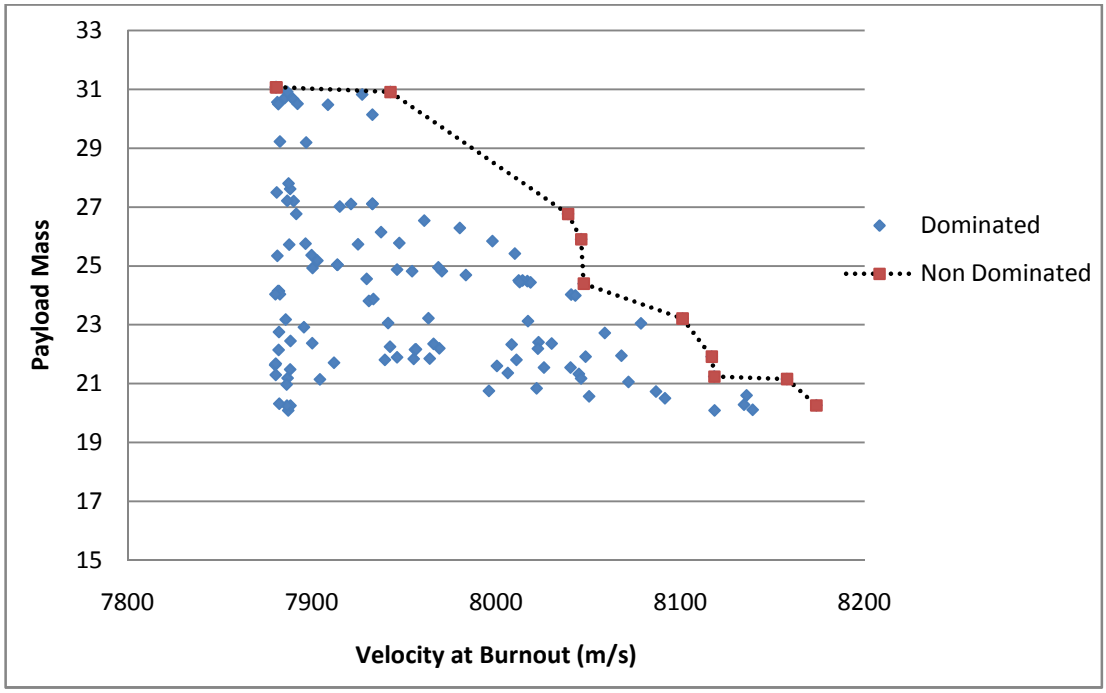

Figure 5-2 Pareto Optimal Front obtained by MC-MOSA with 10,000 function evaluations

Figure 5.2 shows non-dominated solutions for the launch vehicle optimization problem. The Pareto Optimal Front is not smooth as expected. If the number of constraints decrease or penalty coefficients associated with the constraints increase solution converges to a certain region. This results in a more smooth Pareto-Optimal front.

Figure 5-3 – 5-9 shows simulation results of a selected non-dominated solution. Table 5-5 includes values of non dominated points and cost associated with these points.

Table 5-5 Non-Dominated Solutions

Velocity at Burnout	Payload Mass	Cost
7880,25	31,07	3,6276
7880,62	31,07	3,6273
7942,51	30,91	3,6087
8038,90	26.76	3,1245
8046,42	25,91	3,0255
8047,42	24,39	2,8503
8101,12	23,20	2,7156
8116,82	21,91	2,5607
8118,20	21,24	2,4699
8157,74	21,15	2,4764
8173,75	20,26	2,6425

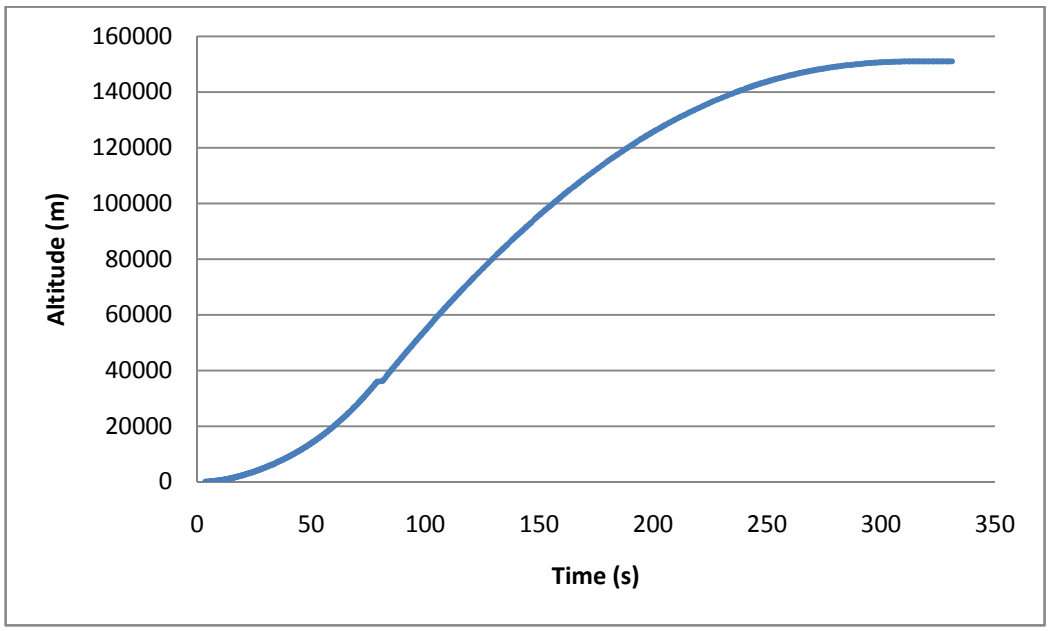

Figure 5-3 Altitude (m) vs. Time (s)

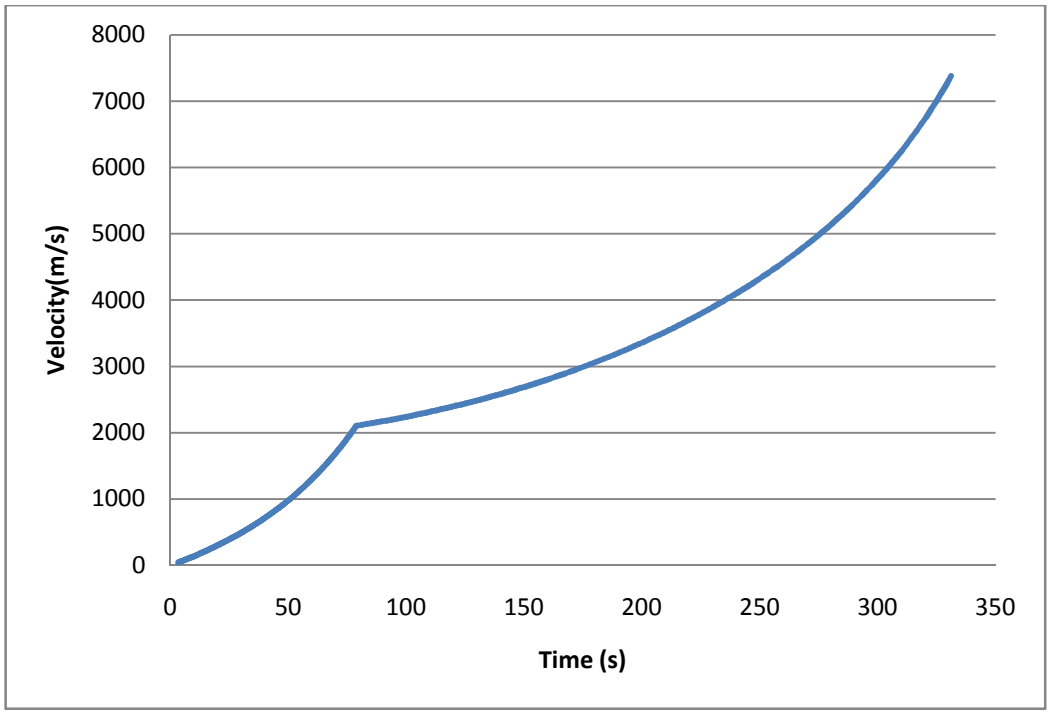

Figure 5-4 Velocity (m/s) vs. Time (s)

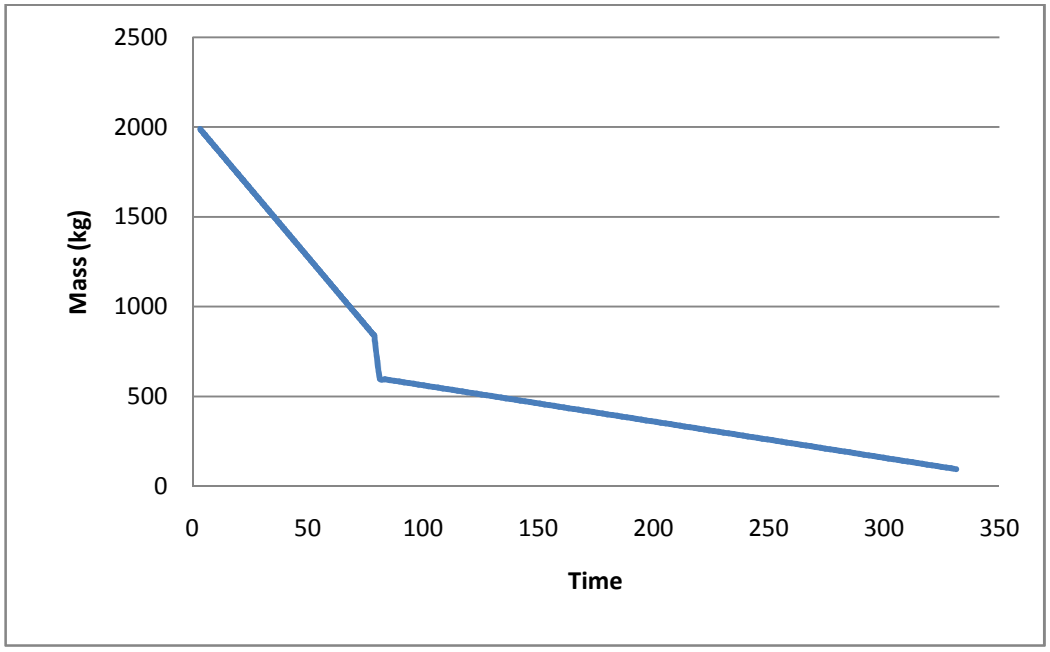

Figure 5-5 Mass vs. Time

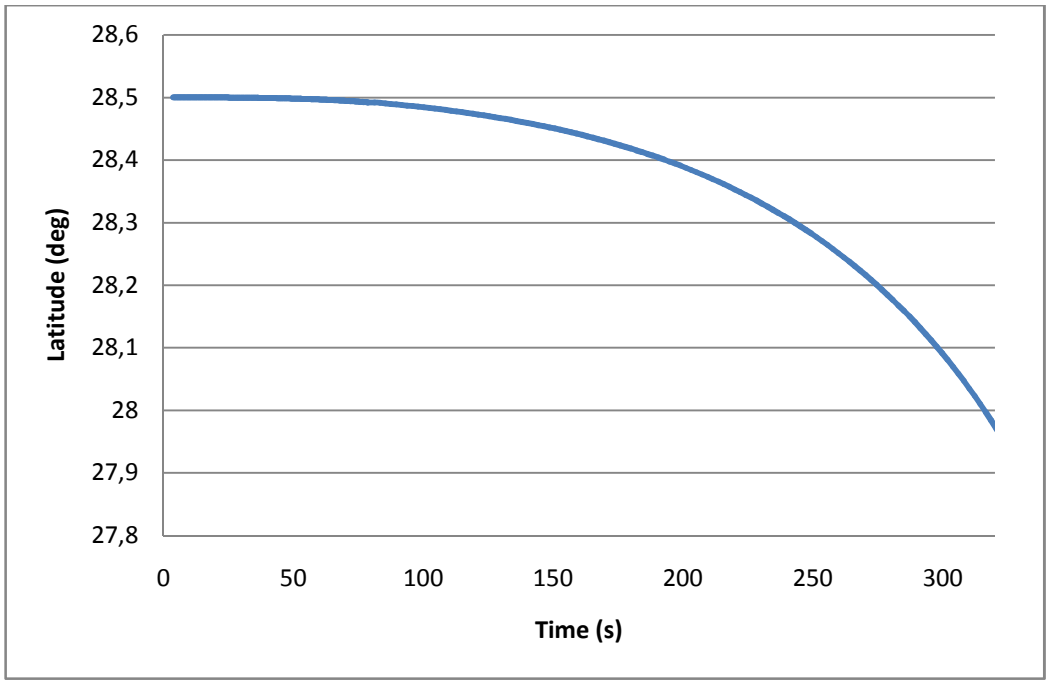

Figure 5-6 Latitude vs. Time

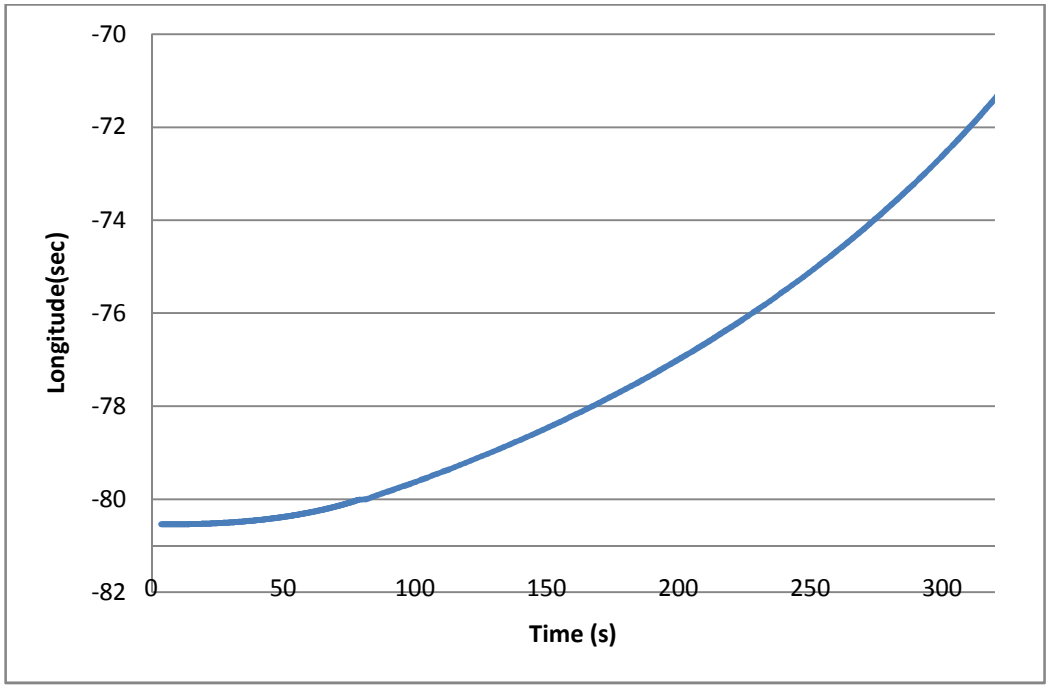

Figure 5-7 Longitude vs. Time

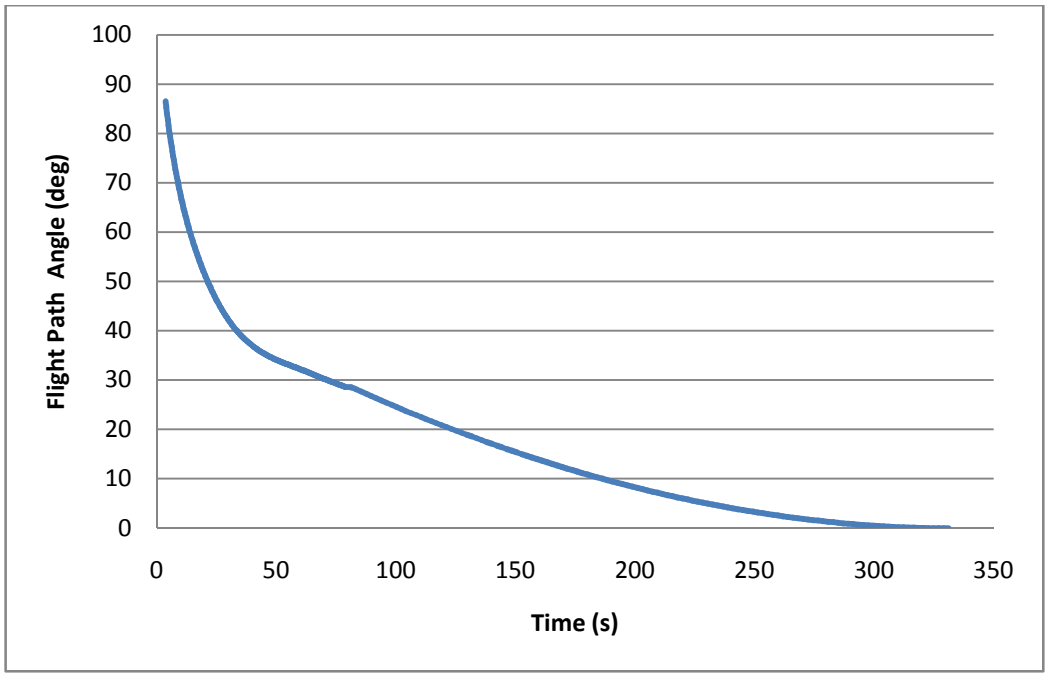

Figure 5-8 Flight Path Angle vs. Time

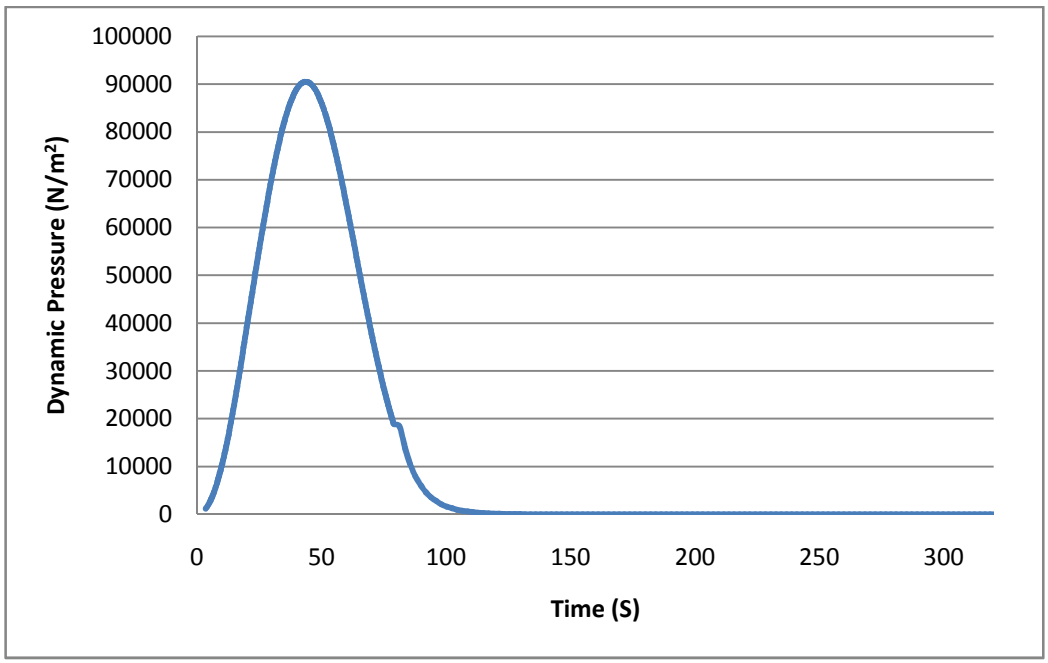

Figure 5-9 Dynamic Pressure vs. Time

5.2.2 Air Launch

In the second scenario launch vehicle is designed where it is launched from F-4 aircraft. When the graphs are compared with the one for the ground

based LV it can be seen that there is less fuel required to achieve ojectives. Moreover, maximum dynamic pressure that the vehicle experiences is far more less than the 1st design. This is due to the fact that the density of air is decreasing in a faster rate although velocity is increasing.

Figure 5-10 Final Design Results for air launched LV

Gross Launch Overall Weight	1485 kg
Weight of 1st stage	1043 kg
Weigt of 1st stage fuel	878 kg
Weight of 2nd stage	442kg
Weigth of 2nd stage fuel	361 kg
ΔV of 1st stage	2854 m/s
ΔV of 2nd stage	5921 m/s
Seperation Time	129. s
Velocity at Burnout	7967.25 m/s
Altitude at Burnout	155587,8 m

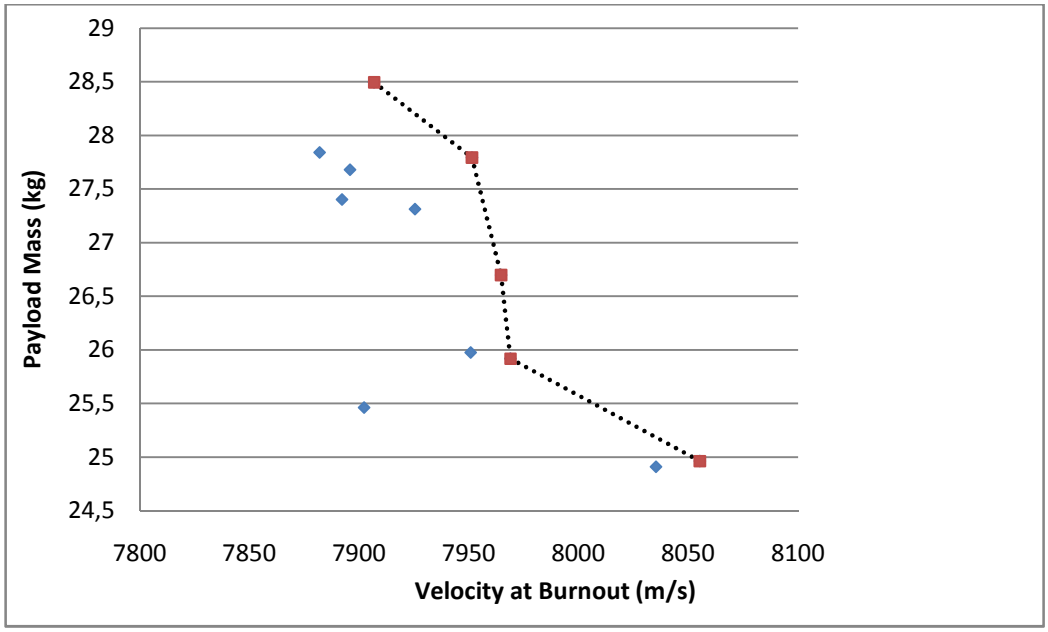

Figure 5-11 Pareto Optimal Front obtained by MC-MOSA for Air Launched-LV Design with 10,000 function evaluations

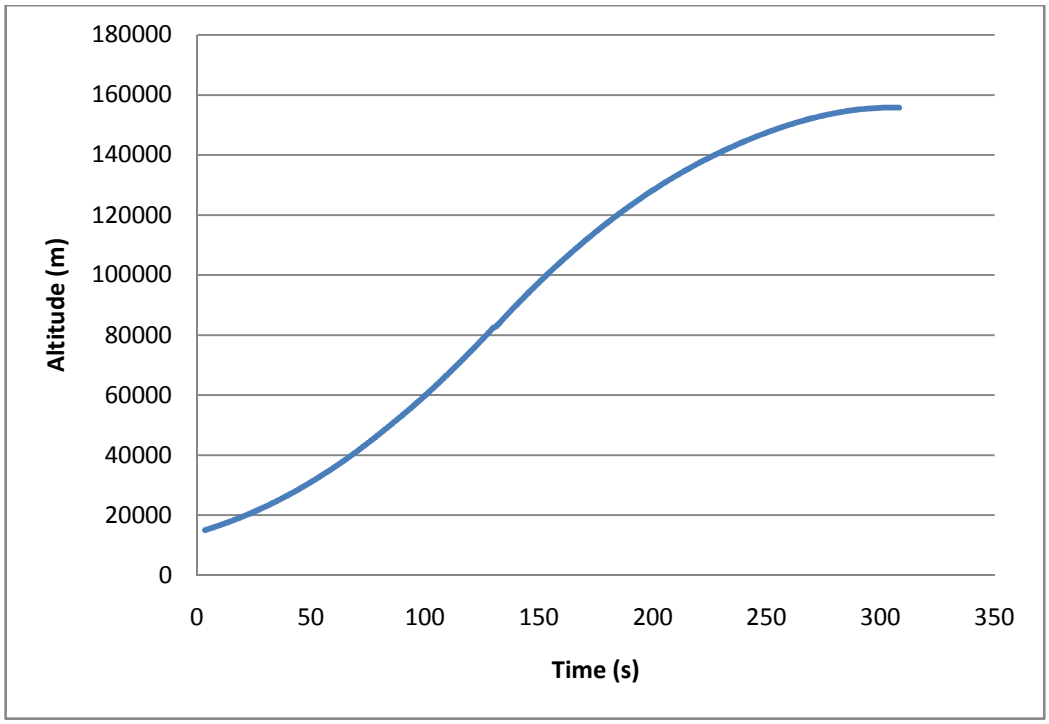

Figure 5-12 Altitude vs. Time graph of Air Launched- LV

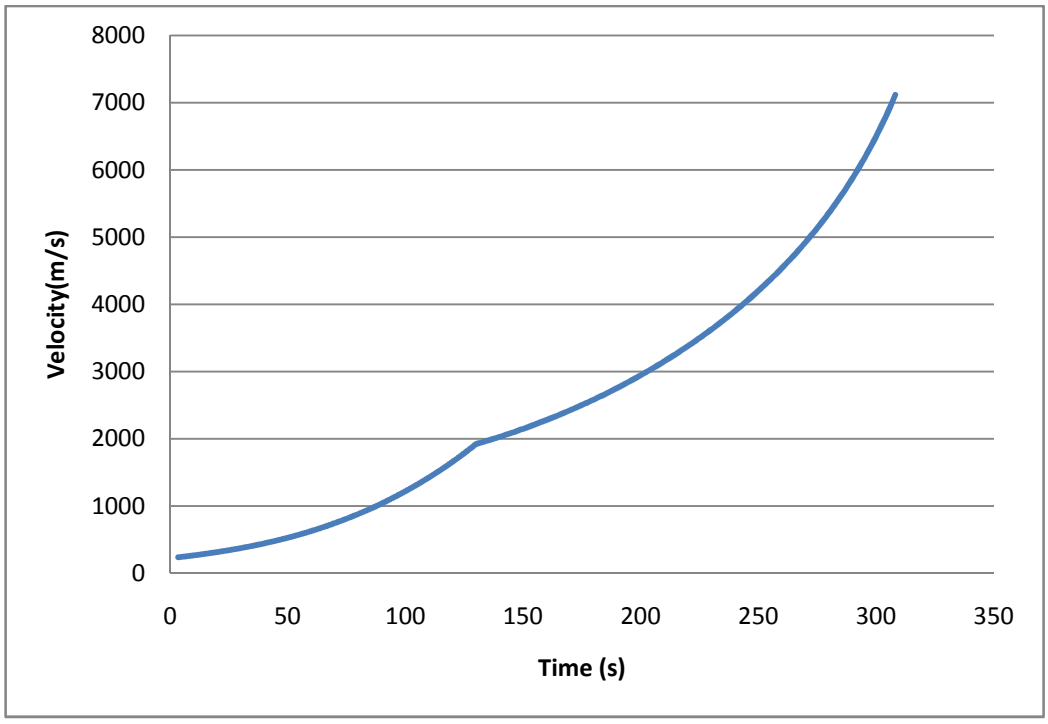

Figure 5-13 Velocity vs. Time graph of Air Launched- LV

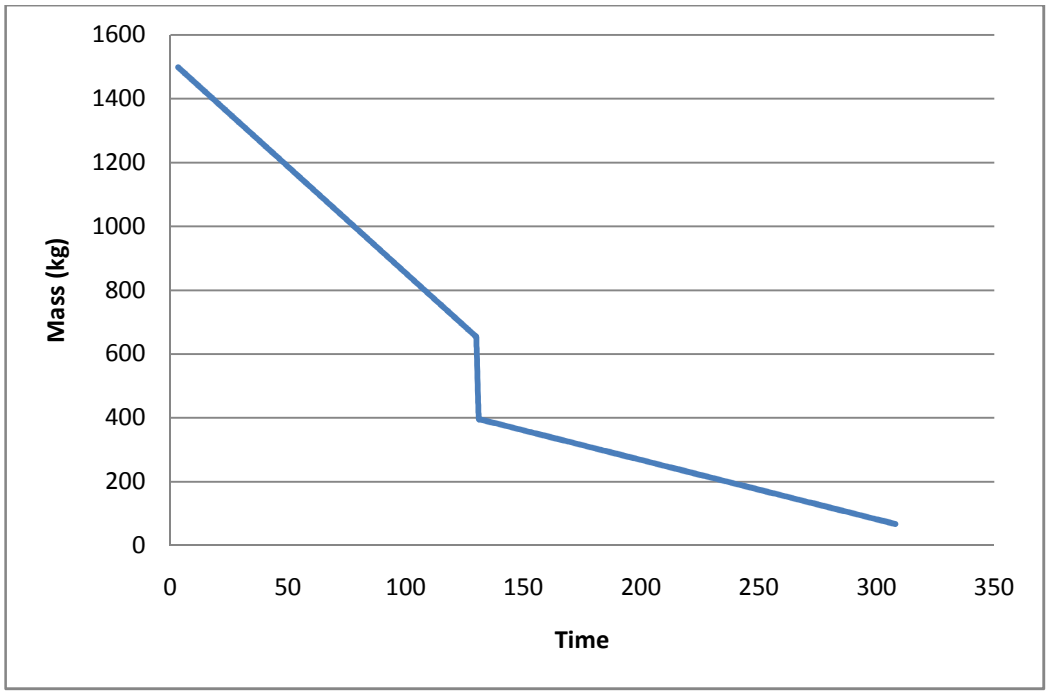

Figure 5-14 Mass vs. Time graph of Air Launched- LV

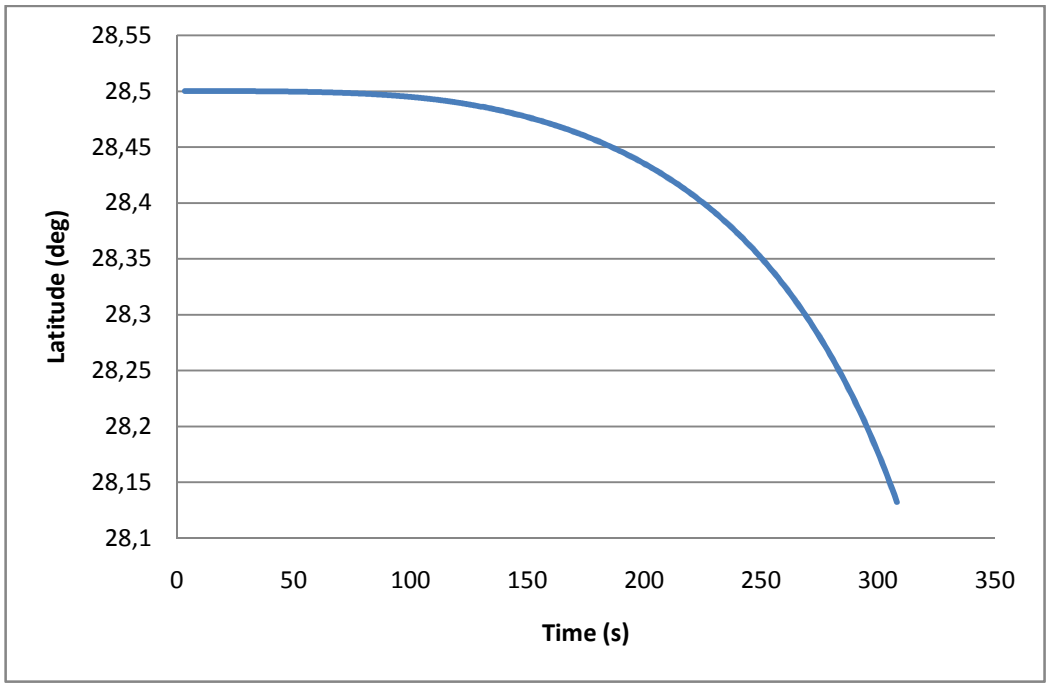

Figure 5-15 Latitude vs. Time graph of Air Launched- LV

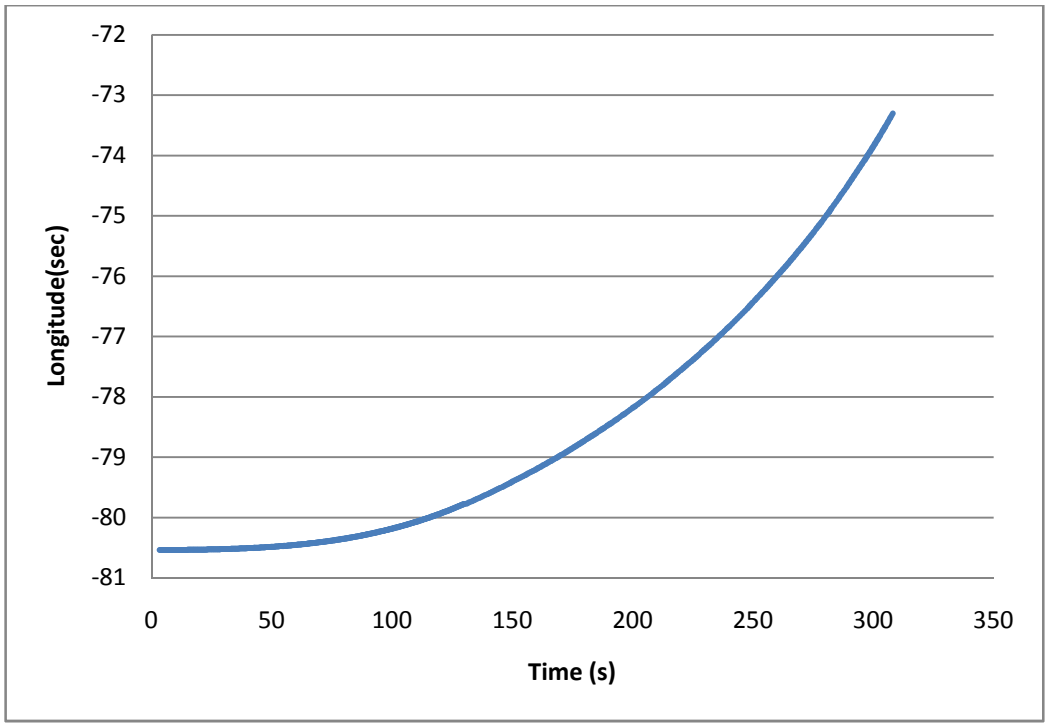

Figure 5-16 Longitude vs. Time graph of Air Launched- LV

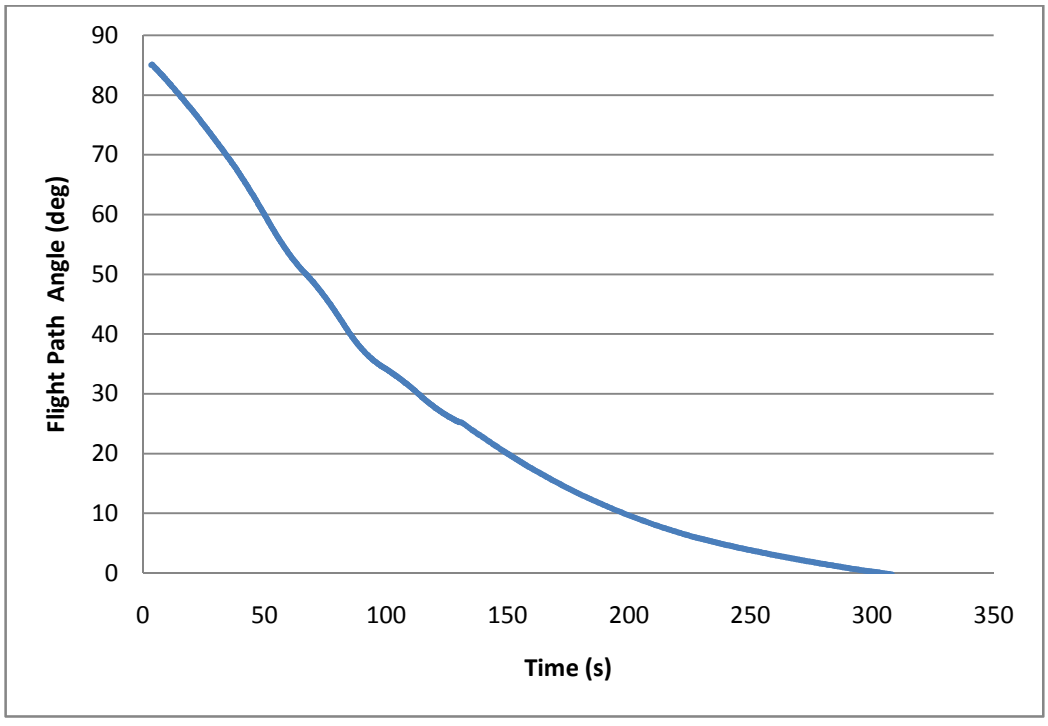

Figure 5-17 Flight Path Angle vs. Time graph of Air Launched- LV

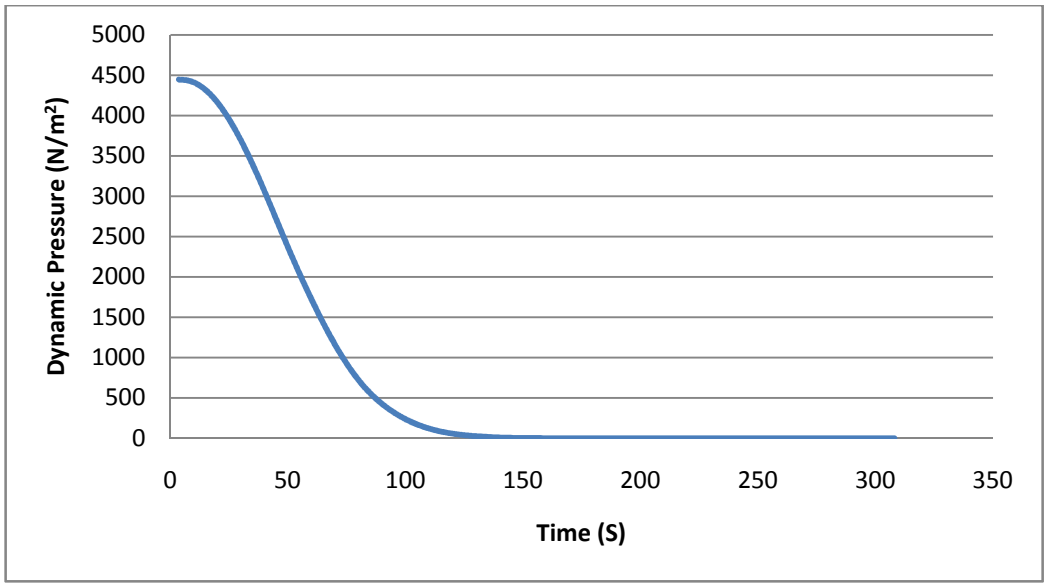

Figure 5-18 Dynamic Pressure vs. Time graph of Air Launched- LV

5.3 Effect of Fitness Function Number

Effect of number of fitness functions is also analyzed. Number of FFs is increased to see the effect on the solution. The solution is obtained for 10k, 30k and 100k function evaluations. It was seen that Pareto-Optimal front is spread on a smaller domain compared to previous case in which number of FFs was 100. The solution obtained with 200FFs and 30k function evaluation numbers (Figure 5.20) is better than the case with 10k function evaluation number (Figure 5.19). Similarly the solution obtained with 100k function evaluation number is better than the previous case. Therefore it can be concluded that the number of function evaluation number results in a better solution.

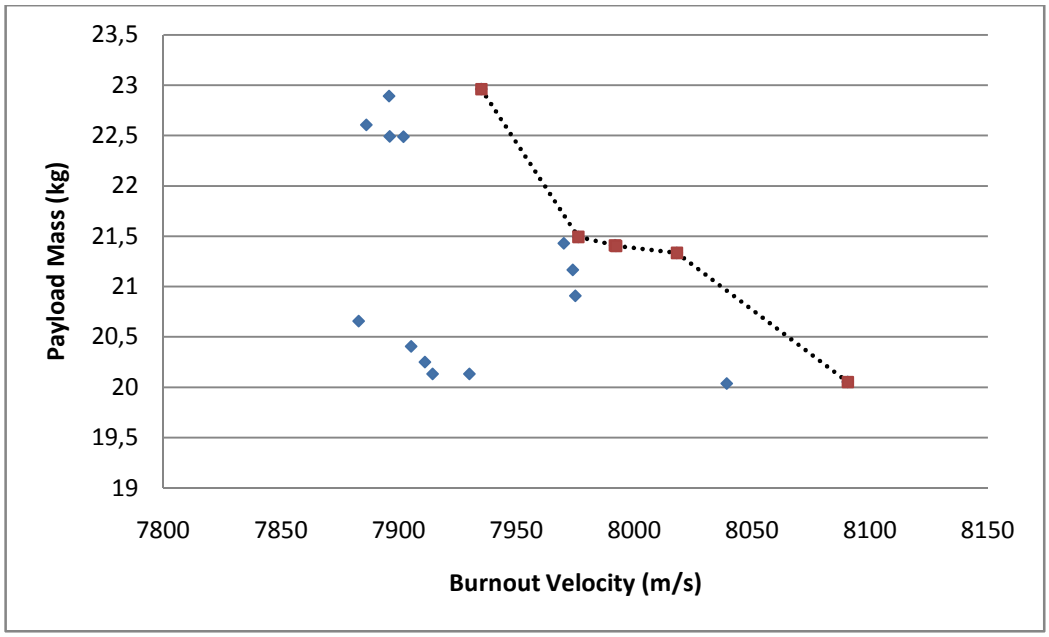

Figure 5-19 Pareto Optimal Front with 200 FFs and 10.000 Function Evaluations

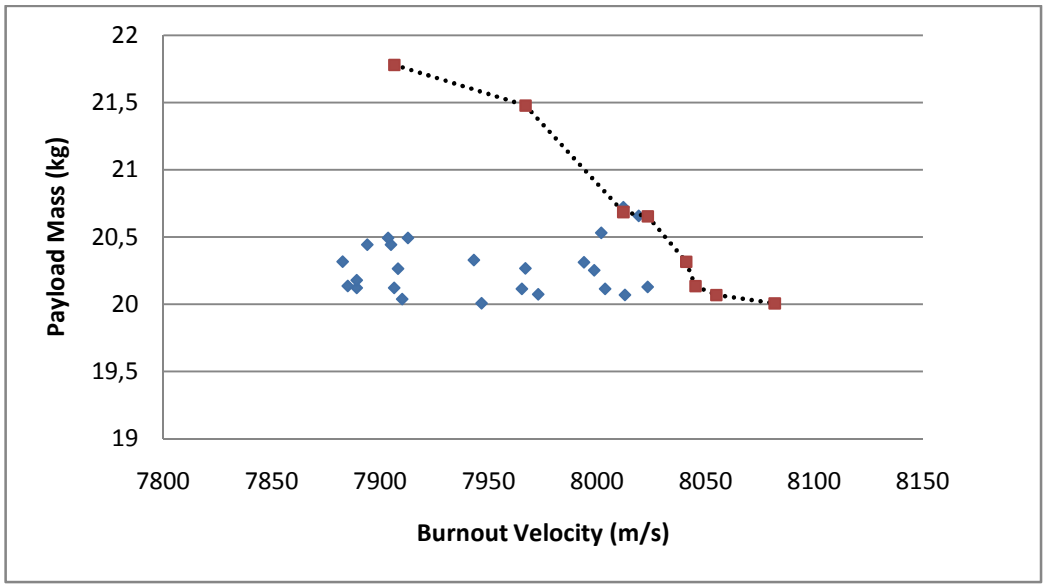

Figure 5-20 Pareto Optimal Front with 200 FFs and 30.000 Function Evaluations

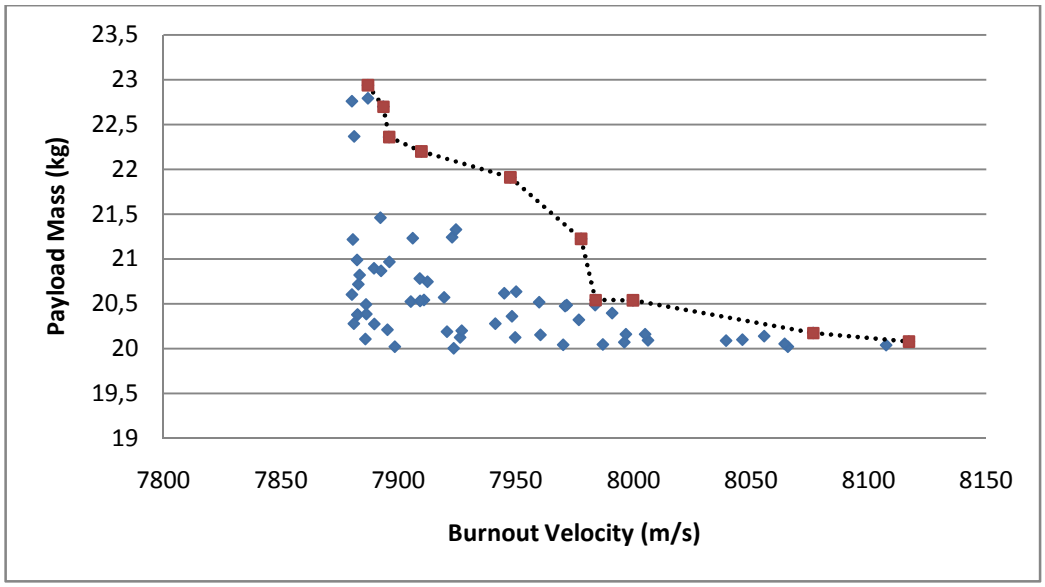

Figure 5-21 Pareto Optimal Front with 200 FFs and 100.000 Function Evaluations

CHAPTER 6

CONCLUSION

In this study past and current satellite technologies are investigated. It was seen that at the beginning of space race first launched satellites were light and small in dimension. Some of these satellites were in the nano-satellite class. However when countries had proven launch technology, these countries launched more capable as well as heavier satellites. The capability and capacity of the launch vehicles are increased together with the satellite technology, and capabilities requested from satellites. With the latest advances in satellite sub-systems smaller satellites could achieve certain tasks that larger satellites were assigned to do so in the past. New concepts were defined and universities and research institutions are also took part in the space arena with national space agencies.

Although number of small satellites designed by the new players increased, there was no dedicated launch vehicle for launching satellites up to 10 kg. This study includes current research in the nano launch vehicle technology. A simple orbit decay calculation was performed to find the target altitude and orbit insertion velocity which was used as objectives in the design phase.

For initial sizing ΔV is found with several assumptions. Later on using optimization parameters optimum path for the launch vehicle is constructed. Initial sizing, engine design and of the launch vehicle was performed again using optimization parameters. Velocity at burnout and payload mass is obtained from simulation of dynamic model of the launch vehicle and analysis described in Chapter 5. The results are used in the optimization phase.

Two scenarios are investigated. In the first case it is assumed that satellite is launched from a ground base. For the second case launch vehicle is integrated onto a F-4 aircraft and launched with an initial velocity and from a certain altitude. It was seen that 2nd scenario get the benefit of initial velocity and altitude hence the mass of the second design was lower compared to the first design as expected.

MC-MOSA algorithm is used for the design optimization of launch vehicle for nano-satellites. Two design cases are used and Pareto-Optimal front for both cases are obtained. The simulated annealing method uses random walk to find the next trial point. The point is used as input to the dynamic model of the launch vehicle and velocity at burnout obtained. If the solution is better than previous one it is accepted. If it does not enhance the solution, acceptance is based on a probabilistic function.

Elliptic fitness functions are used to capture non-convex Pareto-Optimal fronts. Each elliptic function has its own temperature and cooled individually when there is improvement related to the fitness function. Constraints that are related to height, mass and flight path angle are converted into inequality constraints and penalty coefficients are assigned to find the solutions in the desired region. Also quality metrics are used for assessment tool.

Effect of the number of fitness functions are also investigated. It was observed that as the number of fitness functions increase number of non-dominated points decreased. However when function evaluation number is increased the points on the fronts increased as expected.

The study showed that if the problem is not sufficiently constrained there might be more than one solution set that achieves the objectives. Also it is useless to use interpolation method to non dominated points because if one objective is achieved there is no guarantee that the other objective is achieved while satisfying the requirements.

Problems related to the study was mainly due to the design methodology. Some of the formulas were developed for heavier launch vehicles. Therefore when assumptions were not valid, the solution couldn’t obtained. Moreover there is no operational launch vehicle for nano satellites and conceptual design studies in the literature are not parallel. As more study is conducted, more accurate results can be obtained.

In this study the solutions were obtained after permitted number of function evaluations were performed. Final temperature of fitness functions can be deployed as other terminal condition.

REFERENCES

[1] Kirkpatrick, S., et. al., *Optimization by Simulated Annealing*, Science, Vol.220, Number 4598, 13 May 1983

[2] Belisle, C.J.P., et. al., *Hide-and-Seek: A Simulated Annealing Algorithm for Global Optimization*, Department of Industrial and Operations Engineering, Technical Report 90-25, University of Michigan Ann Arbor, 1990

[3] Arslan, E. M., *Optimal Trajectories for Air-toSurface Missiles Using Direct Collocation and Nonlinear Programming*, M.S. Thesis, Aeronautical Engineering Department, METU, Ankara, March 1995

[4] Utalay S.,*Trajectory and Multidisciplinary Design Optimization of Missiles Using Simulated Annealing*, M.S. Thesis, Aeronautical Engineering Department, METU, Ankara, January 2000

[5] Bingöl, M., *Trajectory and Multidisciplinary Design Optimization of Missiles Using Simulated Annealing*, M.S. Thesis, Aeronautical Engineering Department, METU, Ankara, January 2000

[6] Ulungu L. E., et. al., *Heuristic for multi-objective combinatorial optimization problems by simulated annealing, MCDM: Theory and Applications*, Sci-tech, Windsor, pp. 269-278,1995

[7] Ulungu L. E., et. al., *MOSA method: A tool for solving multi-objective combinatorial optimization problems*, Journal of Multi-Criteria Decision Analysis, Vol. 8,pp.221-236,1999

[8] Ulungu L. E., Interactive simulated annealing in a mutiobjective framework: application to a industrial problem, Journal of Operational Research Society, Vol. 49, pp. 1044-1050, 1998

[9] Karslı, G.,*Simulated Annealing for the Generation of Pareto Fronts with Aerospace Applications*, M.S. Thesis, Aerospace Engineering Department,Ankara, January 2004

[10] NASA National Space Science Data Center. http://nssdc.gsfc.nasa.gov/nmc/spacecraftDisplay.do?id=1957-001B. [Access Date: June 2, 2011.]

[11] Explorer 1 Fast Facts. www.jpl.nasa.gov/explorer/facts. [Access Date: April 29, 2011.]

[12] UN Register of Space objects Launched into Outer Space. http://www.unoosa.org/oosa/en/SORegister/docsstatidx.html. [Access Date: 1 June 2011.]

[13] Sandau, R., *Status and trends of small satellite missions for Earth observation*, Acta Astronautica, Vol. 66, pp. 1-12, 2010

[14] Sadin, S. R. , Davis R. W., *The Smallsat Revolution .... Back to the Future?*, Acta Astronautica, Vol: 34, pp. 109-122., 1994

[15] Nakasuka, S., et. al., *Evolution from Education to practical use in University of Tokyo's nano-satellite activities*, Acta Astronautica, 2010, Vol: 66, pp. 1099-1105., 2010

[16] Landsat-1 History . http://landsat.usgs.gov/about_landsat1.php. [Access Date: 6 July 2011]

[17] Gunter's Space Page http://space.skyrocket.de/doc_chr/lau2010.htm [Access Date: 7 May 2011]

[18] UCS Satellite Database http://www.ucsusa.org/ nuclear_weapons_and _global_security/space_weapons/technical_issues/ucs-satellite-database.html [Access Date: 7 May 2011]

[19] Guidebook on Small Satellite Programs, International Space University Summer Studies Program, GoSSP Team Project, 2011

[20] Treaty on Principles Governing the Activities of States in the Exploration and Use of Outer Space, including the Moon and Other Celestial Bodies, United Nations Office of Outer Space Affairs, 1967

[21] Thompson, L. , Nano Satellite Launch Sytem Ausroc Nano, http://www.iafastro.com/docs/2010/iac/nanosat/5_Lachlan.pdf, [Access Date: 15 May 2011]

[22] Charania, A. C., *SpaceWorks Commercial: Nano-Launcher: Dedicated Nanosatellite Payload Delivery Service*, CubeSat Developers' Summer Workshop, Logan-Utah USA, August 2010

[23] Nanolaunch Project**,** http://www.spg-corp.com/nanolaunch-project.html, [Access date: 6 June 2011]

[24] Generation Orbit, http://www.generationorbit.com/ [Access date: 6 June 2011]

[25] The Australian Space Weather Agency, http://www.ips.gov.au/Category/Educational/Space%20Weather/Space%20Weather%20Effects/SatelliteOrbitalDecayCalculations.pdf [Access Date: 1 May 2011]

[26] Shaver, D. A., Hull., D. G., *Advanced Launch System Trajectory Optimization using suboptimal control*, AIAA Guidance Navigation and Control Conference, Portland-USA, pp. 892-901, 1990

[27] Fleeman, E. L., Tactical Missile Design 2nd Edition, 2006

[28] Charoenpon, A., Pankeaw, E., *Method of Finding Aeordynamic Characteristic Equations of Missile for Trajectory Simulation*, World Academy of Science, Engineering and Technology, Vol. 81, 2011

[29] David, P. R., *Analysis of Heavy Lift Launch Vehicle Design Using Small Liquid Rocket Engines*, M.S. Thesis, Massachusetts Institute of Technology, May 1988

[30] Rocket Propellants, http://www.braeunig.us/space/propel.htm [Access Date: 6 July 2011]

[31] Tekinalp, O., Karslı, G., *A new multiobjective simulated annealing algorithm*, Journal of Global Optimization, V. 39, pp. 49-77, 2007

[32] Wu, J., Azarm, S., *Metrics for quality a ssesment of a multiobjective design optimization solution set*, ASME J. Mechanical Design, Vol. 123 pp. 18–25, 2001

[33] Travis S. Taylor, Introduction to Rocket Science and Engineering, 2009

APPENDIX A

Orbital Decay Calculations

Orbital decay algorithm is taken from reference [25]. Following Matlab Code is used in the analysis.

```
%% Orbital Decay Calculation%%

close all
clc

m       =10;     %% mass of the satellite
area    = 0.01;  %% area of the satellite
h       = 300;   %% initial height
f10      = 90;   %% solar radiant flux
ap      = 0;     %% geomagnetic index

re      = 6378000;
me      = 5.98E+24;                 %%Earth radius and mass (all SI units)
g       = 6.67E-11;                 %%Universal constant of gravitation
pi      = 3.1416;
t       = 0;
dt      = 0.1;                      %%time & time increment are in days
d9      = dt * 3600 * 24;           %%put time increment into seconds
h1      = 10;
h2      = h;                        %%H2=print height, H1=print height increment
alt(1)  = h
r       = re + h * 1000;            %%R is orbital radius in metres
p       = 2 * pi * sqrt(r * r * r / me / g);  %%P is period in seconds
i       =1;


while h > 180
        i     =i+1 ;
        sh    = (900 + 2.5 * (f10 - 70) + 1.5 * ap) / (27 - .012 * (h - 200));
        dn    = 6E-10 * exp(-(h - 175) / sh); %%atmospheric density
        dp    = 3 * pi * area / m * r * dn * d9; %%decrement in orbital period

                if h <= h2;  %% test for print
                pm = p / 60; mm = 1440 / pm ; nmm = 1440 / ((p - dp)) / 60; %%print units
                dcy = dp / dt / p * mm; %%rev/day/day
                h2=h2-h1;
                end

p = p - dp; t = t + dt; %% compute new values
r = (g * me * p * p / 4 / pi / pi) ^ .33333; %%new orbital radius
h = (r - re) / 1000 ; %%new altitude (semimajor axis)
```

```
alt(i)= h ;
time(i)=t ;

end

%% now print estimated lifetime of satellite %%

Day=  t
Year= t / 365
plot (time, alt)
hold on
xlabel('Time (Day)')
ylabel('Altitude (Km)')
title('Atmospheric Decay of Nanosatellite')
hold off
```

APPENDIX B

Sample Calculation

The objective is to launch a nano satellite at an altitude of 375 km. Initially ΔV_Pwhich is the ΔV provided by the propulsion system of the launch vehicle should be found.

Actual ΔV

V_{orb}, for low Earth orbit for a circular orbit is;

$$V_{orb} = \sqrt{Gm_{Earth}\left(\frac{2}{r} - \frac{1}{a}\right)} = \sqrt{Gm_{Earth}\left(\frac{1}{r+h}\right)}$$

$$V_{orb} = \sqrt{389601\left(\frac{1}{6378 + 375}\right)} = 7.595\ km/s$$

$$V_{Earth} = \frac{2\pi r}{t} = 463\ m/s$$

And Earth's rotational speed at the latitude of the launch site is;

$$V_{Earth_L} = V_{Earth}\cos\lambda = 463\cos(28.5) = 406.89\ m/s$$

Thus actual ΔV_A is approximated by;

$$\Delta V_A = V_{orb} - V_{Earth_L} = 7595 - 406.89 = 7188.11\ m/s$$

Drag ***ΔV***

$$\Delta V_D = \frac{qS_{ref}C_d}{m}\text{x}\ t = \frac{35000\text{x}1\text{x}0.282}{2000}\text{x}50 = 385.87\ m/s$$

It is assumed that the vehicle is subject to maximum dynamic pressure of *q* for 50 s . Order of magnitude of C_d is 1 and mass is around 2000 kg. Diameter of the launch vehicle is 0.75 m.

Gravity ***ΔV***

Over the course of a flight of duration t_b, this can be approximated as;

$$t_b = \frac{m_{prop}}{\dot{m}}$$

$$Isp = \frac{T}{\dot{m}g} = \frac{Tt_b}{m_{prop}g}$$

To stay in the air $T > m_{prop}g$ so $I_{sp} > t_b$ for any stage. For 2 stage vehicle each having $t_b = \frac{1}{2}I_{sp}$ gives $t_b = I_{sp}$ overall. Hence;

$$\Delta V_G = gt_b\overline{\sin\gamma} = gI_{sp}sp\sin 30 = 9.8\text{x}330\text{x}\sin(30) = 1617\ m/s$$

As a result $\Delta V_p = 7188.11 + 385.75 + 1617 = 9190.86 \cong 9200$

For $\varepsilon = 0.18$, Isp=330 s, n=2

$$\kappa = \frac{\Delta V_P}{cn} = \frac{9200}{9.8x330x2} = 1.42$$

$$\frac{1}{R} = \left(\frac{e^k(1-\varepsilon)}{1-\varepsilon e^k}\right) = 178.07$$

For m_{pay} =11 kg;

$$m_0 = \frac{m_{pay}}{R} = 178.07\text{x}11 = 1958.84\ kg$$